LHCb-PUB-2022-012
March 15, 2022

Future physics potential of LHCb

LHCb collaboration

Abstract

The LHCb experiment has been performing precision measurements of Standard Model parameters and exploring physics beyond the Standard Model. Detector Upgrade I is being implemented and plans for Upgrade II are being formulated. Both upgrades include novel technologies and a unique triggerless data acquisition system. The experiment has been at the cutting edge of not only studies of b and c hadron decays, but also studies of exotic hadron spectroscopy, searches for dark-sector particles, electroweak measurements, and heavy ion collision physics in both colliding beams and fixed-target modes. Several hints of departure from lepton flavor universality have been uncovered. These topics are part of the "Rare Processes and Precision," "Energy," "Instrumentation," and "Computing" frontiers.

For submission to the 2022 Snowmass community planning exercise

Contents

Executive summary

In this document we discuss the physics goals of the LHCb experiment, located at CERN's Large Hadron Collider, and the detector improvements needed to reach those goals. Most importantly, we present the potential for the LHCb experiment to limit or find physics beyond the Standard Model (SM), hereafter referred to as "New Physics" (NP). The LHCb experiment has collected pp collision data corresponding to 9 fb^{-1} of integrated luminosity during Runs 1 (at $\sqrt{s} = 7$ and $8\,\text{TeV}$) and 2 (at $\sqrt{s} = 13\,\text{TeV}$) of the LHC. The detector is currently undergoing an improvement called "Upgrade I" with an expectation of collecting an additional 50 fb^{-1} over an approximately four year period. The Upgrade I detector will begin taking data in 2022. Further Upgrades called Ib and II are now being planned, with the latter planning to collect $300\,\text{fb}^{-1}$.

The sensitivity of various NP searches will be improved in each upgrade step. These include investigations using mixing and CP violation in b and c hadrons, a broad program of studies of lepton flavor universality in b-hadron decays, searches for dark matter in dark photon conversions and certain b decays, and lepton flavor violation. Other important physics aspects include measurements of SM parameters such as CKM matrix elements, electroweak studies, exotic hadron spectroscopy, and the full centrality range of heavy ion collisions.

LHCb has been successful in making many first measurements in the field of flavor physics including the discovery of CP violation in charm meson decays, best in the world measurements using B decays including $\mathcal{B}(B^0_s \to \mu^+\mu^-)$, the CKM angle γ, and the CP violating angle called ϕ_s in $B^0_s \to J/\psi\phi$ and $J/\psi\pi^+\pi^-$ decays. We have also discovered pentaquark and tetraquark states, and have seen many new conventional meson and baryon states.

Many aspects of the LHCb physics program have been covered in detail in the 2018 submission to the European Strategy for Particle Physics, "Physics case for an LHCb Upgrade II - Opportunities in flavour physics, and beyond, in the HL-LHC era" [1]. The detector aspects of the proposed Upgrade Ib and II program are discussed in full detail in the "Framework TDR for the LHCb Upgrade II" [2]. In order to cope with the anticipated more than 40 interactions per crossing and the high radiation dose at the Upgrade II environment, most subdetector elements will either be completely replaced or undergo major improvements, including the addition of timing measurements in most subsystems. In this document we add selected new results and outline ideas for the future detector upgrades.

The LHCb program touches on several Snowmass frontiers including "Rare Processes and Precision," "Energy," "Instrumentation," and "Computing" frontiers.

1 Introduction

New Physics may influence the decays of particles containing the b and c quarks through the presence of as yet undiscovered particles and interactions in quantum loops. These effects can be ascertained by several methods including deviations from the Standard Model predictions of the decay branching fractions, angular distributions, or CP asymmetries, depending on the decay mode under observation. The mass scales probed in this manner go up to 10^5 TeV, depending on the specific model [3], much higher than can be accessed in direct production.

During Runs 1 and 2 of the LHC, LHCb has produced a number of world-best measurements of this type. These include the branching fraction of the extremely rare decay $B_s^0 \to \mu^+\mu^-$ [4], and the measurement of the CKM unitarity triangle angle γ [5]. The unique capabilities of LHCb can also lead to unexpected discoveries. One example is the test of lepton flavor universality in the ratio of flavor changing neutral current decays $R(K) = \mathcal{B}(B^+ \to K^+\mu^+\mu^-)/\mathcal{B}(B^+ \to K^+e^+e^-)$ [6], which with $9\,\mathrm{fb}^{-1}$ of data collected during LHC Runs 1 and 2 deviates from the SM prediction by 3.1σ. LHCb has also performed a broad program of studies of lepton flavor universality in the semileptonic $b \to c\ell\nu$ transition. Combined with the first measurements of these quantities at BaBar and those at Belle, these results are in 3.4 σ tension with the SM. A consistent pattern of anomalies in these and related measurements supplies evidence for new physics. Other examples of novel phenomena that LHCb has investigated include the first observation of CP violation in the charm sector [7], searches for dark photons [8], and lepton flavor violation [9]. While LHCb has already produced excellent results in these areas, all of these studies will benefit greatly from larger data samples. LHCb has also observed for the first time a large number of hadronic states, both conventional and exotics such as tetra- and pentaquarks. But this is only the beginning, as the sensitivity of these measurements will continue to increase with orders of magnitude more data [1].

Increased data can be obtained on a reasonable time scale through a series of detector upgrades that allow for running with an order of magnitude higher instantaneous luminosity. The Upgrade I detector is being installed now [10–16], and will operate during LHC Runs 3 and 4, with a goal to collect $50\,\mathrm{fb}^{-1}$ of data. Further upgrades are proposed for LHC long shutdown three (Upgrade Ib), and long shutdown four (Upgrade II) [2], with a total target of $300\,\mathrm{fb}^{-1}$.

The components of Upgrade I are sketched in Fig. 1. The most important detector improvements are the new tracking system and the read out architecture that allows the use of a purely software trigger that enables data to be taken at five times the previous rate with the acceptance of purely hadronic b decays increased by up to a factor of two. The VErtex LOcator (VELO) is based on pixelated-silicon sensors and is critical to determining vertices of b and c flavored hadrons. The upstream tracker, UT, contains vertically-segmented silicon strips and continues the tracking from the VELO. It is also used to determine the momentum of charged particles to $\Delta p/p \approx 10\%$, extremely useful to remove low momentum tracks from being extrapolated downstream, thus speeding up the software trigger by about a factor of three. Tracking after the magnet is supplied by the scintillating fiber based SciFi detector. Two Ring Imaging CHerenkov (RICH) detectors supply particle identification. RICH1 is mainly for lower momentum particles and RICH2 is for higher momentum ones. The ECAL identifies electrons and reconstructs photons and neutral pions. The HCAL and M2-M5 are mostly used for muon identification. The

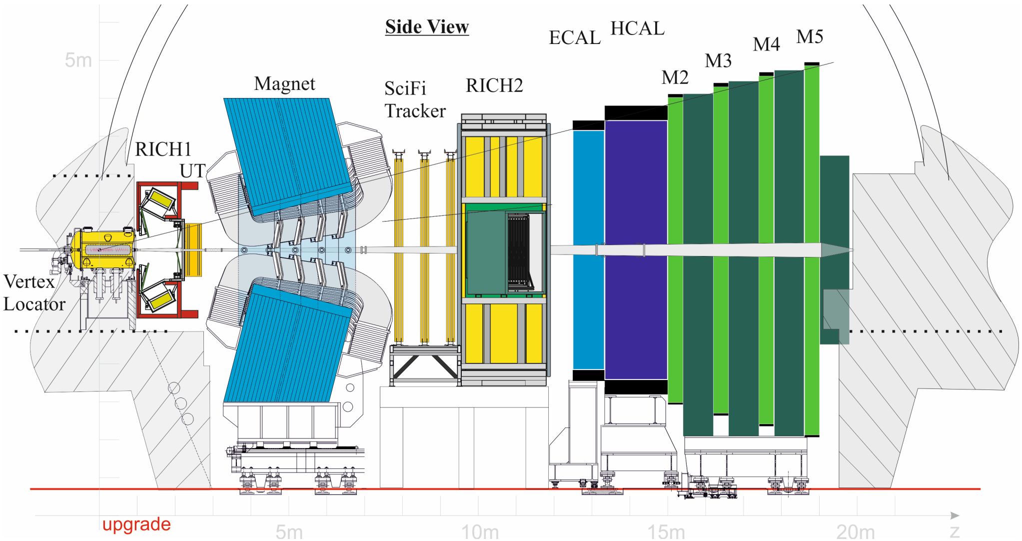

Figure 1: Sketch of the Upgrade I LHCb detector. All of the detector elements have been modified to output data at the beam crossing rate of 40 MHz without the use of hardware trigger. Not shown is the new software trigger framework.

US groups are mainly involved with the UT silicon-based tracking detector, and with the online triggering and data taking.

The Upgrade Ib changes will improve the tracking acceptance and particle identification capabilities. There are several important changes that already have had substantial R&D. Tracks that are on the lower end of the momentum spectrum are bent into the sides of the magnet and not reconstructed. Placing chambers on the side magnet faces to measure where they hit the magnet allows a measurement of their momenta with as good, or better, resolution as tracks that go through the entire system [17], increasing efficiencies in many decay modes and searches, and expanding access to the low (x,Q^2) region of the nucleus in proton+ion and ion+ion collisions.

In Upgrade II, the main goals are to operate the experiment at up to a factor of 7 higher instantaneous luminosity and use new detector concepts to sustain and extend the capabilities of the LHCb detector. This will require the addition of timing measurements to many of the detector subsystems. The upgraded detector will also allow access to the full range of centrality in ion+ion collisions. The detector improvements proposed for Upgrade II, and the technological R&D needed, are discussed in more detail in section 3.

Upgrade II of the LHCb detector will be able to access a very wide range of flavor observables and measure them with unprecedented precision. The expected uncertainties for a few key measurements with $300\,\text{fb}^{-1}$ are presented in Table 1. Also shown are the current uncertainties, those expected from LHCb just before the start of the HL-LHC era, and for Belle II, which is due to complete operation around this time. In addition, and where available, sensitivity estimates are given for ATLAS and CMS after their Phase-II Upgrades and with $3000\,\text{fb}^{-1}$ of data. Further discussion of the Upgrade II physics program is found in section 2.

Table 1: Summary of prospects for future measurements of selected flavour observables for LHCb, Belle II and Phase-II ATLAS and CMS. The projected LHCb sensitivities take no account of potential detector improvements, apart from in the trigger. The Belle-II sensitivities are taken from Ref. [18]. This table is adapted from [1], using updated values available in [2].

Observable	Current LHCb	LHCb 2025	Belle II	Upgrade II	ATLAS & CMS
EW Penguins					
R_K $(1 < q^2 < 6\,\mathrm{GeV}^2c^4)$	0.044 [6]	0.025	0.036	0.007	–
R_{K^*} $(1 < q^2 < 6\,\mathrm{GeV}^2c^4)$	0.12 [19]	0.031	0.034	0.009	–
CKM tests					
γ	$4°$ [5]	$1.5°$	$1.5°$	$0.35°$	–
$\sin 2\beta$, with $B^0 \to J/\psi K^0_S$	0.04 [20]	0.011	0.005	0.003	–
ϕ_s, with $B^0_s \to J/\psi\phi$	32 mrad [21]	14 mrad	–	4 mrad	22 mrad [22]
ϕ_s, with $B^0_s \to D^+_s D^-_s$	170 mrad [23]	35 mrad	–	9 mrad	–
$\phi_s^{s\bar{s}s}$, with $B^0_s \to \phi\phi$	154 mrad [24]	39 mrad	–	11 mrad	Under study [25]
a^s_{sl}	33×10^{-4} [26]	10×10^{-4}	–	3×10^{-4}	–
$\lvert V_{ub}\rvert/\lvert V_{cb}\rvert$	6% [27]	3%	1%	1%	–
B^0_s, $B^0 \to \mu^+\mu^-$					
$\mathcal{B}(B^0 \to \mu^+\mu^-)/\mathcal{B}(B^0_s \to \mu^+\mu^-)$	69% [4, 28]	41%	–	11%	21% [29]
$\tau_{B^0_s \to \mu^+\mu^-}$	14% [4, 28]	8%	–	2%	–
$S_{\mu\mu}$	–	–	–	0.2	–
$b \to c\ell^-\bar{\nu}_l$ LUV studies					
$R(D^*)$	0.026 [30, 31]	0.007	0.005	0.002	–
$R(J/\psi)$	0.24 [32]	0.07	–	0.02	–
Charm					
$\Delta A_{CP}(KK - \pi\pi)$	29×10^{-5} [7]	13×10^{-5}	5.4×10^{-4}	3.3×10^{-5}	–
A_Γ $(\approx x \sin\phi)$	11×10^{-5} [33]	5×10^{-5}	3.5×10^{-4}	1.2×10^{-5}	–
Δx $(D^0 \to K^0_S\pi^+\pi^-)$	18×10^{-5} [34]	6.3×10^{-5}	–	1.6×10^{-5}	–

2 Recent physics results and future expectations

Since the release of Ref. [1], a number of new LHCb results have been published which further demonstrate the sensitivity of the LHCb detector to a wide range of physics processes. They help to establish a baseline for extrapolating the full reach of Upgrade II at the HL-LHC. An outline of the key physics areas of the Upgrade-II and a number of new results are discussed in more detail in this section.

2.1 *CP* violation

A necessary condition for the baryon asymmetry of the Universe (BAU) is the violation of *CP* symmetry [37]. The level of *CP* violation in the CKM matrix, with just a single *CP*-violating phase, is orders of magnitude too small to account for the BAU observed today. New physics (NP) can introduce new particles and mediators, which can in turn contribute additional complex amplitudes to specific decays, which may involve new

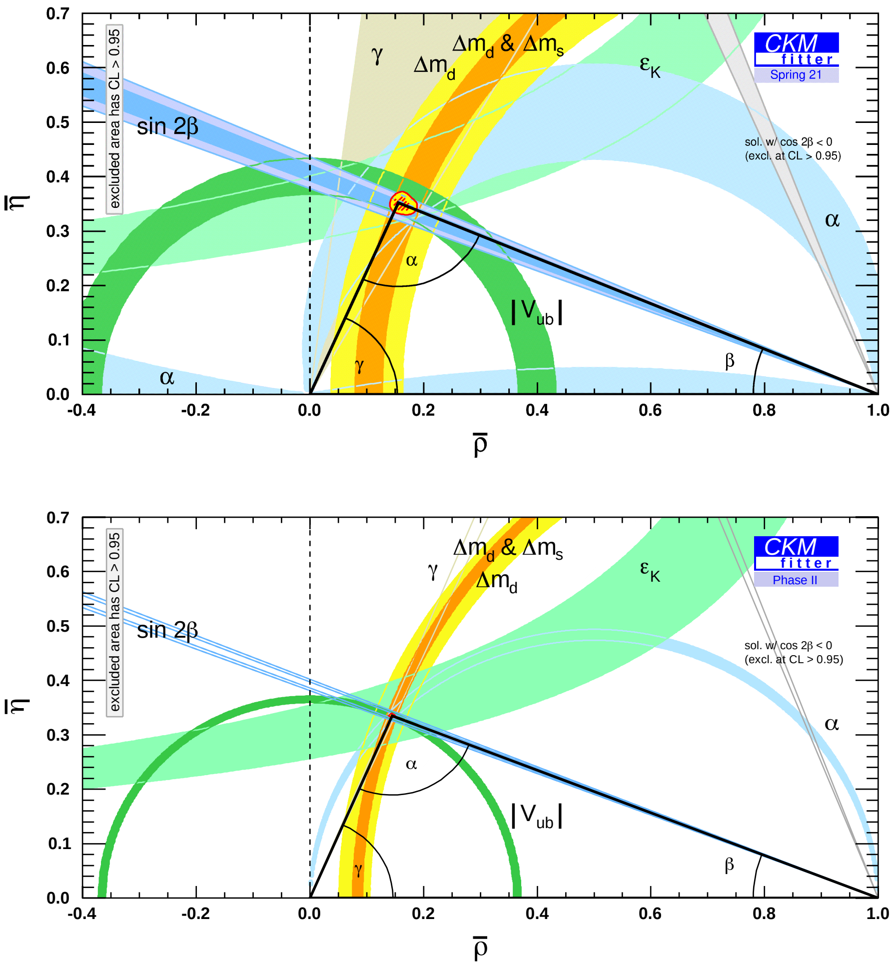

Figure 2: Constraints in the $\bar{\rho}-\bar{\eta}$ plane from LHCb measurements and lattice QCD calculations (top) as of Spring 2021, and (bottom) with the anticipated improvement with 300 fb^{-1} of data collected by LHCb (assuming unitarity) [35, 36] and anticipated reductions in the uncertainties in hadronic factors from Lattice QCD.

CP-violating phases. Probing the CKM paradigm through precise measurements of *CP* violation in heavy flavor decays is therefore of fundamental importance to uncovering NP, which may help with understanding the BAU.

A program of measurements over the last 20 years or so has led to the constraints on the unitarity triangle shown in Fig. 2(top). The non-zero value of the apex of the triangle in the $(\bar{\rho}, \bar{\eta})$ plane is due to the aforementioned weak phase in the CKM matrix. The apex can be probed in a number of processes, and, if the SM is correct, all such measurements should give a consistent value. Any discrepancy between the apex obtained in the study of different processes would be an indication for new physics. Generally, *CP* violation measurements fall into one of two categories, time-integrated and time-dependent, the status of which are briefly discussed below.

2.1.1 Time-integrated *CP* violation

The study of the decay $B^{\mp} \to DK^{\mp}$, and similar decays, allows for a theoretically clean determination of the weak phase γ. The D meson is in a superposition of D^0 or $\overline{D}^0$ meson states, corresponding to the quark-level transitions $b \to c\bar{u}s$ and $b \to u\bar{c}s$, respectively. Several D final states are accessible to both D^0 and $\overline{D}^0$ mesons, and the interference between the $b \to c\bar{u}s$ and $b \to u\bar{c}s$ transitions directly probes the weak phase γ. The modes that provide the greatest sensitivity to γ include $K^0_S\pi^+\pi^-$ [38], K^+K^- and $\pi^+\pi^-$ [39] and $K^{\mp}\pi^{\pm}$ [40, 41]. Because these modes occur at tree-level (no loop processes), the value of γ obtained in such decays is expected to be uninfluenced by the presence of new physics.

The most recent result from LHCb, which includes 15 decay modes, yields $\gamma = (65.4^{+4.2}_{-3.8})^{\circ}$ [5]. The determination of γ from these modes is theoretically clean, and therefore the uncertainties are driven by the sample sizes and control over the systematic uncertainties. Due to the very nature of the measurements, e.g. asymmetries involving *CP* conjugate final states, systematic uncertainties often cancel, or are small and experimentally quantifiable with control samples. Moreover, as larger samples of charm decays are collected (by both LHCb and BES III), uncertainties related to charm meson input parameters will decrease as well. The statistical errors will clearly decrease as the sample sizes increase. With the samples collected through Upgrade II, LHCb anticipates an ultimate precision on γ of about 0.35°. Figure 2(bottom) shows the level of precision on γ expected with $300\,\mathrm{fb}^{-1}$ of data collected with the Phase II upgrade.

2.1.2 Time-dependent *CP* violation in B^0 and B^0_s mixing

Additional constraints on the unitarity triangle enter through the measurement of B^0 and B^0_s mixing, which are mediated by second-order box diagrams involving heavy virtual top and $W^{\pm}$ bosons. Additional massive particles could contribute, and modify these amplitudes. Both the magnitude and the relative phase between the mixing and decay amplitudes are experimentally accessible, which probe the CKM elements V_{td} and V_{ts}.

The magnitude $|V_{td}/V_{ts}|$ is related to the ratio of mixing frequencies, $\Delta m_d/\Delta m_s$ by SM constants and hadronic matrix elements. Currently the uncertainties on these hadronic factors is dominant, and therefore a reduction in the theoretical uncertainties, e.g. from Lattice QCD, is needed before improved measurements of Δm_s and Δm_d can make an impact on $|V_{td}/V_{ts}|$. Fortunately, such improvements in the relevant matrix elements using Lattice QCD are anticipated in the future [35], which would allow a considerable shrinking of the constraints coming from $B_{(s)}$ mixing.

The phase of B^0 mixing gives a clean determination of $\sin(2\beta)$, where β is the phase associated with the CKM element V_{td} and corresponds to the right lower corner angle in the unitarity triangle in Fig. 2. The current uncertainty on $\sin(2\beta)$ from LHCb is 0.04 [20] using $B^0 \to J/\psi K^0_S$ decays collected with a $3\,\text{fb}^{-1}$ data sample. Since the systematic uncertainty is about an order of magnitude lower than the statistical uncertainty, larger data samples will lead to a decrease in the uncertainty in $\sin(2\beta)$ for quite some time. With the full Upgrade II sample, LHCb anticipates an uncertainty on $\sin(2\beta)$ of about 0.003, as shown in Fig. 2(bottom). This uncertainty is comparable to that expected from the full Belle II data sample.

The phase associated with B^0_s mixing in the Standard Model is expected to be very small, $\phi_s = -2\arg(-V_{ts}V^*_{tb}/V_{cs}V^*_{cb}) = -36.5^{+1.3}_{-1.2}$ mrad [42]. Any measurement that deviates significantly from this small value would be an indication of NP in B^0_s mixing. The most precise measurements of ϕ_s are obtained from the time-dependent flavor-tagged decay rates of $B^0_s \to J/\psi K^+K^-$ and $B^0_s \to J/\psi\pi^+\pi^-$ decays. With about 1/3 of the 13 TeV data sample, LHCb measures $\phi_s = -83 \pm 41 \pm 6$ [21] and $\phi_s = 2 \pm 44 \pm 12$ [43] mrad for the $B^0_s \to J/\psi K^+K^-$ and $B^0_s \to J/\psi\pi^+\pi^-$ modes, respectively. Both measurements are consistent with the SM and will be statistically limited for the foreseeable future. With the full Upgrade II samples, a precision of about 4 (6) mrad is expected from $B^0_s \to J/\psi K^+K^-$ ($B^0_s \to J/\psi\pi^+\pi^-$), far better than any other experiment. LHCb has also measured ϕ_s in $B^0_s \to D^+_s D^-_s$, and this mode is expected to achieve a sensitivity of about 9 mrad with the full Upgrade II sample. The anticipated precision on ϕ_s is promising to either reveal new physics or place very tight constraints on NP contributions [35].

An additional measurement that can prove interesting with larger LHCb data samples is the *CP*-violating phase in $B^0_s \to \phi\phi$ decays. The SM expectation for this phase, $\phi_s^{s\bar{s}}$ is very small, about 0.02 rad [44–46]. Unlike in $B^0_s \to J/\psi K^+K^-$, $J/\psi\pi^+\pi^-$ decays, the $B^0_s \to \phi\phi$ decay occurs only at loop level, and so NP may enter into the decay amplitude. The current value of $\phi_s^{s\bar{s}}$ is $-0.17 \pm 0.15 \pm 0.03$ rad [24]. With the full Upgrade II sample, a precision of about 0.01 rad is expected. The decay $B^0_s \to \overline{K}^{*0}K^{*0}$ is also promising to determine $\phi_s^{d\bar{d}}$ [47], which has the advantage that one can also analyze the U-spin related decay $B^0 \to \overline{K}^{*0}K^{*0}$ to control theoretical uncertainties. With the full Upgrade II sample, a precision of 0.009 (0.035) rad on $\phi_s^{d\bar{d}}$ is expected for $B^0_s \to (K^-\pi^+)(K^+\pi^-)$ ($B^0_s \to \overline{K}^{*0}K^{*0}$) [1].

2.2 Measurement of the CKM elements $|V_{ub}|$ and $|V_{cb}|$

The parameters $|V_{ub}|$ and $|V_{cb}|$ remain the subject of intense theoretical and experimental scrutiny. They affect the precision determination of the “standard” unitarity triangle. In addition, a precise determination of $|V_{cb}|$ has a strong impact on the interpretation of experimental measurements of rare decays such as $B^0_s \to \mu^+\mu^-$ ($|V_{cb}|^2$), $K^+ \to \pi^+\nu\bar{\nu}$ ($|V_{cb}|^3$), and $K^0 \to \pi^0\nu\bar{\nu}$ ($|V_{cb}|^4$) [48].

A strong theoretical effort is ongoing to achieve ever increasing precision on the prediction of the matrix elements necessary to extract these fundamental observables from measured quantities. In particular, effects of radiative corrections are being considered [49], improved lattice QCD calculations continue to be made available [50], and parameters of the heavy quark expansion used to interpret inclusive measurements are determined up to higher orders in the QCD perturbative expansion [51].

While experiments such as LHCb and Belle have provided measurements of increasing precision, the major source of uncertainty remains the tension between inclusive and exclusive determinations, namely whether a specific decay mode such as $B^0 \to D^{*-}\mu^+\nu_\mu$ is used, or an inclusive property such as the muon spectrum from B^0 semileptonic decays. The tension between these two determinations of the better known parameter $|V_{cb}|$ is still at the 3σ level [52]. The strength of LHCb in these measurements is the variety of hadrons that can be studied. For example, a measurement of the ratio $|V_{ub}|/|V_{ub}|$ was performed by LHCb using semileptonic b-baryon decays [27]. The planned detector improvements in Upgrade II will significantly enhance the opportunities for $|V_{ub}|$ extraction with decays such as $B_s^0 \to K^-\mu^+\nu_\mu$, which has also been recently observed by LHCb [53]. The larger data sample will allow study of semileptonic decays of the B_c^+ mesons, of great theoretical interest. These are only some examples of the broad program accessible to advance our knowledge of these fundamental SM parameters.

2.3 Lepton flavor universality

A fundamental assumption within the SM is that the electroweak couplings to the three known generations of fermions are identical, a symmetry called *Lepton Flavor Universality* (LFU). As a result, the only differences expected among observables that involve leptons of different generations are due to their different masses. Deviations from LFU would thus be powerful indications of NP. Interestingly, a series of measurements over the last decade of decays involving $b \to s\ell\ell$ ($\ell = e, \mu$) [54–64] and $b \to c\tau\nu$ [31, 32, 65–71] transitions have resulted in 2–3σ discrepancies with respect to their SM predictions, see Fig. 3. These measurements include LFU ratios[1] such as $\mathcal{R}_{H_s} = \frac{\mathcal{B}(H_b \to H_s\mu\mu)}{\mathcal{B}(H_b \to H_s ee)}$ and $\mathcal{R}(H_c) = \frac{\mathcal{B}(H_b \to H_c\tau\nu)}{\mathcal{B}(H_b \to H_c\ell\nu)}$, in which some of the experimental and theoretical uncertainties, common to the numerator and denominator, cancel. On their own, most of the current individual results have low significance deviations from the SM, but these deviations follow a remarkably consistent pattern. The decays involving $b \to s\mu\mu$ generally are found to have lower rates than expected whereas those from $b \to c\tau\nu$ transitions tend to exceed the SM expectation.

LHCb is in an excellent position to shine light on this puzzle thanks to its unique combination of vertexing and particle identification capabilities together with the large number of b-hadrons produced at the LHC. This is especially true in the case of the rare $b \to s\ell\ell$ decays; since 2018, LHCb has reported:

- the first deviation from the SM of more than 3σ in a single LFU observable ($\mathcal{R}_{K^+}$) [54],
- the first measurement of an LFU ratio involving baryons ($\mathcal{R}_{pK}$) [57],
- the first observations of $B \to K_S^0 ee$ and $B \to K^{*+} ee$ together with the LFU ratios $\mathcal{R}_{K_S^0}$ and $\mathcal{R}_{K^{*+}}$ [79],
- the angular distributions of $B \to K^*\mu\mu$ [58, 59], $B_s \to \phi\mu\mu$ [80], and $\Lambda_b \to \Lambda\mu\mu$ [81],
- the differential branching fractions of $B_s \to \phi\mu\mu$ and $B_s \to f_2'(1525)\mu\mu$ as a function of the invariant mass of the lepton pair, q^2 [63].

[1] Here and in the rest of this section, $\ell = e, \mu$ and $H_{b,c,s}$ are generic b-, c-, and $s-$hadrons, respectively.

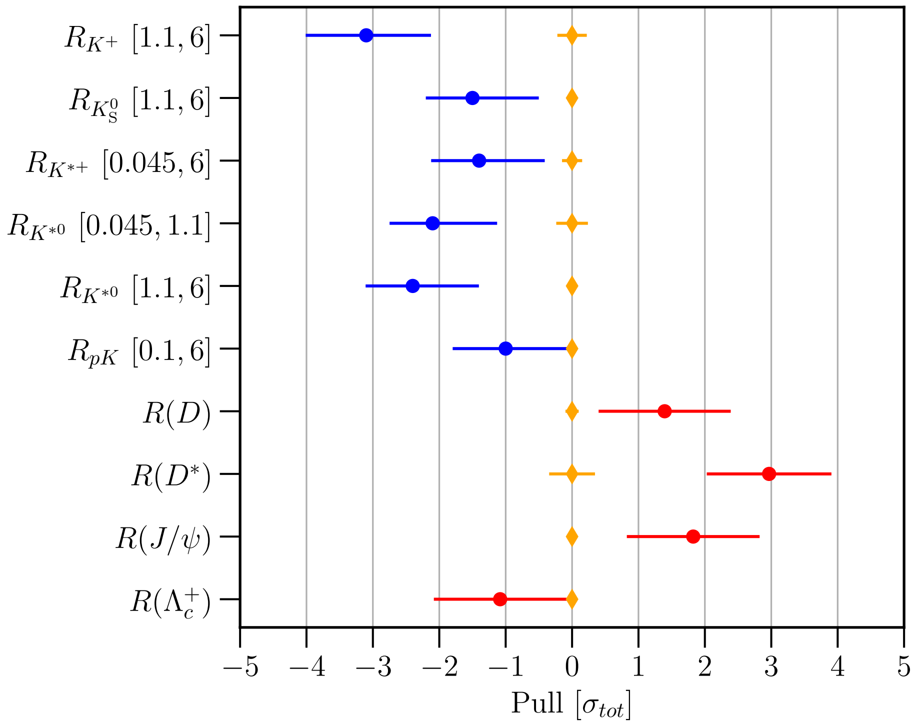

Figure 3: Compatibility of measurements [31, 32, 54–62, 64–71] of LFU-related observables $\mathcal{O}$ with the corresponding SM predictions [72–77] as quantified by their pulls. The pulls are defined as $(\mathcal{O}_{\text{exp}} - \mathcal{O}_{\text{th}})/\sigma_{\text{tot}}$, where σ_{tot} combines the total experimental and theoretical uncertainties in quadrature. The uncertainties shown on the markers illustrate how much of σ_{tot} comes experiment versus from theory. If a significance is given in the relevant publication, this value is used instead of the computed significance. Markers in blue (red) correspond to decays involving $b \to s\ell\ell$ ($b \to c\tau\nu$) transitions, while markers in orange indicate the theoretical predictions, which zero pulls with respect to themselves. The numbers in brackets correspond to the q^2 range of the measurement. The values of $\mathcal{R}(D)$ and $\mathcal{R}(D^*)$ are the current world averages [76]. Adapted from Ref. [78].

The large data samples expected after Upgrades I and II will allow the LHCb measurements of LFU observables to reach 1%-level uncertainties [82] . This precision would be sufficient to establish or reject the level of LFU violation seen in the current measurements. Additionally, these data samples will also allow for the measurement of the related $b \to d\ell\ell$ transitions. For example, the statistical precision on $\mathcal{R}_\pi$ with the full Upgrade II dataset is expected to reach a few percent.

Decays involving $b \to c\tau\nu$ transitions are more challenging due to the multiple unreconstructable neutrinos in the final state. The B-factories have performed the most precise measurements of $\mathcal{R}(D)$ and $\mathcal{R}(D^*)$ to date thanks to their ability to significantly constrain the kinematics of these neutrinos by leveraging their knowledge of the e^+e^- collision energy. LHCb, however, is expected to surpass the B-factories precision and reach uncertainties down to the percent level [83] from the analysis of the enormous data samples expected from the operation of the Upgrades I and II detectors, provided that the relevant systematic uncertainties can be properly controlled. Additionally, a key advantage of LHCb is the ability to measure LFU ratios for b-hadrons other than B mesons. In 2017, LHCb published the measurement of $\mathcal{R}(J/\psi)$ [84], the first LFU result in B_c^+ decays, and they recently made public the first measurement of $\mathcal{R}(\Lambda_c^+)$ [85]. The uncertainties are fairly large, for now, but the precision on these and other observables not yet measured such as $\mathcal{R}(D_s^{(*)})$ and $\mathcal{R}(D^{**})$ are expected to improve quickly thanks to the Upgrade I and II datasets [83].

Finally, the large Upgrade datasets will also allow for the measurement of kinematic distributions that are very sensitive to BSM physics [86–88]. LHCb should be able to measure key angular observables in $B \to K^*\mu\mu$ [86] and is capable of resolving the three angles that describe $B \to D^*\tau\nu$ decays [89]. Since the measurement of these distributions would be affected by different sources of uncertainty than those the LFU ratios are subject to, they could be instrumental in providing a robust and complete view on $b \to s\ell\ell$ and $b \to c\tau\nu$ transitions as well as in characterizing any possible BSM physics.

2.4 Leptonic decays

Similarly to the $b \to s\ell\ell$ decays discussed in the previous section, the fully leptonic $B^0_{(s)} \to l^+l^-$ decays (with $l = e, \mu, \tau$) proceed via loop-mediated flavor-changing neutral currents. However, the additional helicity suppression in leptonic decays further decreases their SM branching fractions by one to two orders of magnitude, a feature that makes these decays extremely sensitive to potential NP contributions. Moreover, the calculation of their decays rates involves one single Wilson coefficient and only one hadronic constant that is already known to 0.5%, so that the SM expectations for the leptonic branching fractions are understood to the 4–5% level in the case of electrons and muons [77], and to 6–9% in the case of tau leptons [90]. The ratios $\mathcal{B}\left(B_s^0 \to l^+l^-\right)/\mathcal{B}\left(B^0 \to l^+l^-\right)$ are known even more precisely with uncertainties of the order of 2%.

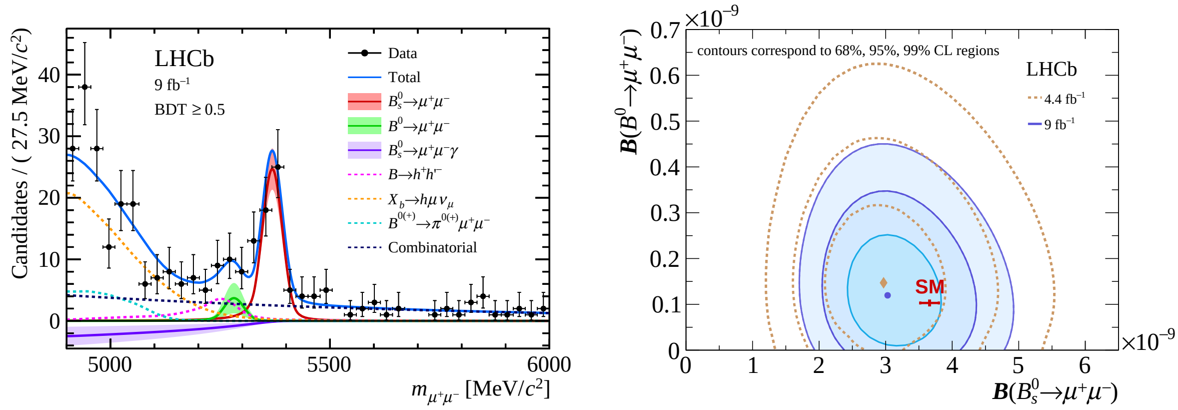

Figure 4: Measurement of $B^0_{(s)} \to \mu^+\mu^-$ decays by LHCb [91, 92]. Left: Mass distribution of signal candidates for values of the classification BDT larger than 0.5. Right: comparison of the measured branching fractions and the corresponding SM predictions [77].

The experiments at the LHC are especially well suited to measure the $B^0_{(s)} \to \mu^+\mu^-$ channel given the very rare nature of these decays and clean final state. The latest measurements from ATLAS [93] and CMS [94], based on partial Run 2 datasets, saw significances for their $B_s^0 \to \mu^+\mu^-$ signals of about 5σ. The 2021 measurement by LHCb based on the full Run 1+2 dataset [91, 92] found $\mathcal{B}\left(B_s^0 \to \mu^+\mu^-\right) = \left(3.09^{+0.46+0.15}_{-0.43-0.11}\right) \times 10^{-9}$ and $\mathcal{B}\left(B^0 \to \mu^+\mu^-\right) = \left(1.20^{+0.83}_{-0.74} \pm 0.14\right) \times 10^{-10}$ with 10.8σ and 1.7σ signal significances, respectively. As shown in Fig. 4, these results are compatible with the SM predictions. However, when combined with the measurements from ATLAS and CMS, the $B^0_{(s)} \to \mu^+\mu^-$ rate is 2.3σ too low and consistent with the deviations seen in the $b \to s\mu\mu$ results discussed above. The LHCb measurement [91, 92] also included results for the effective lifetime of $B^0_{(s)} \to \mu^+\mu^-$, $\tau^{\text{eff}}_{\mu\mu} = 2.07 \pm 0.29 \pm 0.03$ ps, and the upper limit $\mathcal{B}\left(B^0_s \to \mu^+\mu^-\gamma\right) < 2.0 \times 10^{-9}$ at 95% for $m_{\mu\mu} > 4.9$ GeV.

LHCb has also established the most stringent upper limits for the other, more challenging leptonic decays. Using the three-prong decays of τ leptons, LHCb set upper limits in 2017 [95] based on a third of the Runs 1+2 dataset of $\mathcal{B}\left(B^0 \to \tau^+\tau^-\right) < 2.1 \times 10^{-3}$ and $\mathcal{B}\left(B^0_s \to \tau^+\tau^-\right) < 6.8 \times 10^{-3}$, both at 95% confidence level and about five orders of magnitude above the SM expectations. For the electron channel, LHCb set limits in 2020 [96] of $\mathcal{B}\left(B^0 \to e^+e^-\right) < 3.0 \times 10^{-9}$ and $\mathcal{B}\left(B^0_s \to e^+e^-\right) < 1.1 \times 10^{-8}$, also at 95% confidence level and five orders of magnitude above the SM expectations.

Since the precision of all of these measurements is completely dominated by statistical uncertainty, the large data samples expected from the operation of the Upgrade I and II detectors will provide significant discovery potential. With the 300 fb^{-1} to be collected after Upgrade II, the sensitivity to the electron and tau decays will improve by more than a factor of five, $B^0 \to \mu^+\mu^-$ should be firmly established, and the ratio $\mathcal{B}\left(B^0_s \to \mu^+\mu^-\right)/\mathcal{B}\left(B^0 \to \mu^+\mu^-\right)$ could be measured with a 10% uncertainty. The only result that may be limited by its systematic uncertainty is $B^0_{(s)} \to \mu^+\mu^-$, where the current 15% uncertainty is projected to be reduced to 1.8%. The current systematic uncertainty is 4.8%, dominated by the uncertainties on the fragmentation fraction f_s/f_d (3.2% as measured by LHCb in 2021 [97]) and on $\mathcal{B}\left(B^+ \to J/\psi K^+\right)$ (2.4% [98]). Thus, taking full advantage of the Upgrade II sample will require further improvements on the measurements of those quantities as well as on the theoretical expectations.

Additionally, the Upgrade I and II datasets will allow LHCb to precisely measure $\tau^{\text{eff}}_{\mu\mu}$ and the time-dependent CP asymmetry of $B^0_{(s)} \to \mu^+\mu^-$ decays, leading to stringent constraints on the parameters $A^{\mu\mu}_{\Delta\Gamma}$ and $S_{\mu\mu}$ [99]. These parameters are very sensitive to BSM contributions, and their measurement helps reduce the uncertainties in the branching fraction measurement.

2.5 Lepton flavor violation

Lepton flavor violating decays are predicted by many theoretical models attempting to explain lepton flavor universality results [100–105]. Since the Upgrade II physics case, several results have been produced using Run 1 and Run 2 data which validate the sensitivity of the LHCb experiment to these processes. A search for the decays $B^+ \to K^+\mu^\pm e^\mp$ [9] using Run 1 data set limits at 90% CL for $K^+\mu^-e^+$ at $< 7.0 \times 10^{-9}$ and for $K^+\mu^+e^-$ at $< 6.4 \times 10^{-9}$. Given the small background level observed, it is expected that these limits can be reduced by more than an order of magnitude through the Upgrade II era.

For decays with τ leptons, limits were set for $\mathcal{B}(B^0_{(s)} \to \tau^\pm\mu^\mp) < 1.4(4.2) \times 10^{-5}$ at 95% CL, using the decay $\tau^+ \to \pi^+\pi^-\pi^+\nu_\tau$ [106] using Run 1 data. A first result with Run 2 data for the decay $B^+ \to K^+\mu^-\tau^+$ using $B^{*0}_{s2} \to B^+K^-$ decays [107], allowing the use of inclusive τ decays, was obtained with an upper limit set at 3.9×10^{-5} at 90% CL, just above the previous result from BaBar [108]. These searches are expected to improve with more data at approximately the square root of the luminosity, which may give sensitivity below 10^{-6} in some cases.

2.6 Charm physics

The enormous production rate of charmed hadrons at the LHC has allowed the LHCb experiment to perform a broad set of fundamental measurements in the charm system, including D^0 mixing parameters, constraints on *CP* violation in mixing and searches for *CP* violation in charmed hadron decays. The physics reach of this program will be significantly enhanced with the much larger data sets expected from the operation of the Upgrade I and Upgrade II detectors. The fully software trigger of the upgraded experiment will allow for the collection of orders of magnitude larger samples of charmed hadrons than any other experiment, including Belle II. The addition of the magnet stations would further boost the efficiency of selecting flavor-tagged decays, crucial for the studies of mixing and *CP* violation.

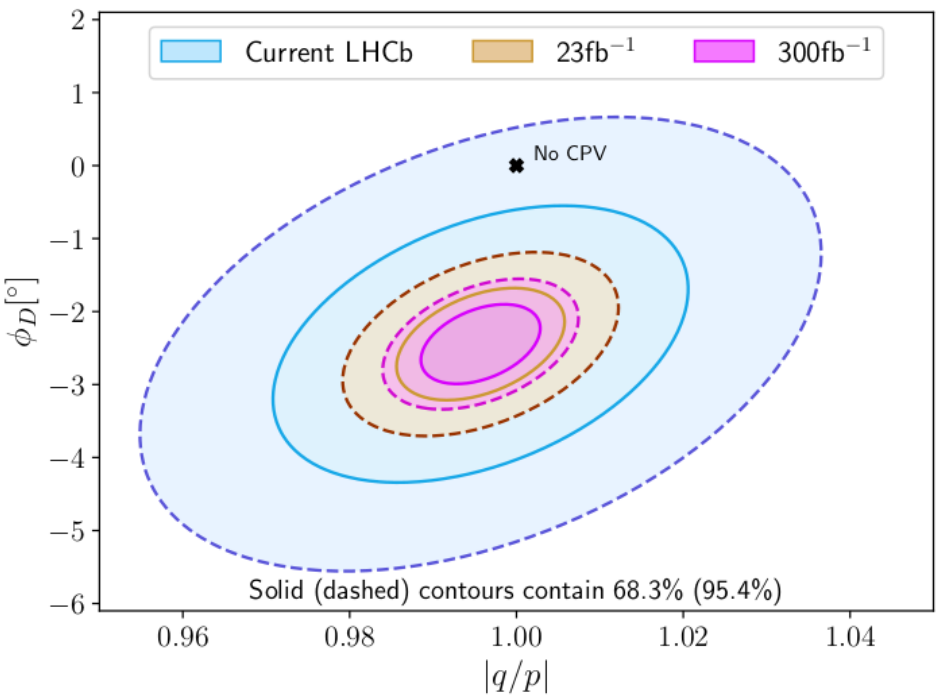

Figure 5: Projected sensitivity with LHCb Upgrade II to the parameters of *CP* violation in charm mixing, $|q/p|$ and ϕ_D, assuming the current central values of experimental observables. Contours shaded with different darknesses indicate 68.3% and 95.4% confidence levels, corresponding to 1 and 2 sigma respectively.

Within the SM, mixing and *CP* violation in the charm sector are predicted to be extremely small, the latter of order $O(10^{-4})$. This provides an opportunity for searching for the influence of NP that may result in significant enhancement of these effects. Until recently, observed *CP* violation was confined to the kaon and b-hadron systems. LHCb has performed the first observation of *CP* violation in charm decays using the measured asymmetry parameter ΔA_{CP} [7]. This result, which is consistent with the upper end of the SM predictions, also represents the first observed *CP* violating effect in the u-type quark sector. LHCb has also performed precise measurements of mixing parameters, allowing constraints on the *CP* violation parameters $|q/p|$ and ϕ_D. Although current results show no evidence for *CP* violation in mixing, with the projected sensitivities of Upgrade II, shown in Fig. 5, LHCb will have the best sensitivity of any planned experiment for observing *CP* violation in mixing.

2.7 Strange physics

The strange hadron production cross-section at the LHC exceeds 1 barn [109, 110], and approximately 20% of the kaons and hyperons produced at the LHCb interaction point are within the geometrical acceptance of the spectrometer. The efficiency of detecting strange hadron decays is, however, not the same as for heavy flavour because of their large flight distances and the low transverse momentum of their decay products.

During the first run of the LHC, no dedicated kaon triggers were available at LHCb, leading to a total trigger efficiency at the order of 1% for the $K^0_S \to \mu^+\mu^-$ decays that would have otherwise been reconstructed. Despite a total reconstruction and trigger efficiency of $\sim 10^{-4}$, LHCb provided two world-best results on rare strange decays: an upper limit on the $K^0_S \to \mu^+\mu^-$ branching fraction thirty times more precise than the previous value [111], and an evidence for $\Sigma \to p\mu^+\mu^-$ [112] with a branching fraction compatible with the HyperCP evidence [113], although with no sign of an anomalous dimuon invariant mass. For the rest of the second run of the LHC, improvements in the trigger increased the trigger efficiency by about an order of magnitude from $\sim 2\%$ to $\sim 20\%$ [114]. This further improved the upper limit on $\mathrm{BR}(K^0_S \to \mu^+\mu^-)$ by yet another factor of four [115], yielding a final result $\mathcal{B}(K^0_S \to \mu^+\mu^-) < 2.1 \times 10^{-10}$ at 90% confidence level. More measurements of kaon and hyperon decays may also be possible.

The LHCb Upgrade II detector, with a purely software trigger, will provide efficiencies nearly one order of magnitude bigger than those in Run 2. The future capabilities of the LHCb upgrades for strange physics have been documented in [110]. LHCb has, in particular:

- a sensitivity in the branching fraction of $K^0_S \to \mu^+\mu^-$ close to the SM prediction;
- world best measurements in rare K^0_S decays such as $K^0_S \to \pi^0\mu^+\mu^-$, $K^0_S \to 4\ell$ (with $\ell = e$ or μ), $K^0_S \to X^0\mu\mu$, or $K^0_S \to X^0\pi\mu$, where X^0 is any neutral system;
- measurements in rare K^+ decays, which could compete with NA62 on some channels such as $K^+ \to \pi^+\mu^+\mu^-$ and similar fully charged final states;
- precise measurements of FCNC decays $\Sigma^+ \to p\mu^+\mu^-$ and $\Sigma^+ \to pe^+e^-$ with tests of lepton flavor universality;
- measurements of *CP* violation in both charged and neutral hyperon decays (the latter from cascade decays);
- searches for new physics in kaon and hyperon decays, such as lepton flavor or baryon number violating decays.

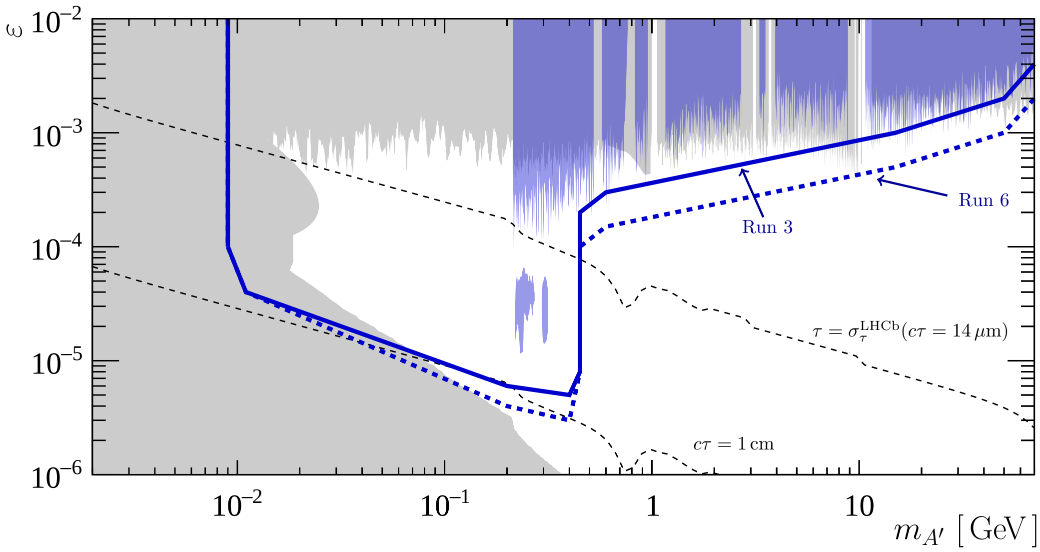

Figure 6: Adapted from Ref. [116]: constraints on visible A' decays from (blue regions) LHCb [118] and (gray regions) all other experiments. The solid blue line is the union of Run 3 projections for LHCb from Refs. [117, 119], along with more recent unpublished inclusive $A' \to e^+e^-$ projections based on 2018 data. The dashed blue line projects further into the future to the end of Run 6.

2.8 Dark sectors

The possibility that dark matter particles may interact via unknown forces, felt only feebly by Standard Model particles, has motivated substantial effort to search for dark-sector forces. LHCb has produced world-leading results using data collected in Runs 1 and 2, and will have greatly enhanced discovery potential in this area after its upgrades.

2.8.1 Dark photons

Recently, substantial effort has been dedicated [116] to searching for a massive *dark photon*, A', whose small coupling to the electromagnetic current arises due to kinetic mixing between the SM hypercharge and A' field strength tensors. Constraints have been placed on visible A' decays by previous beam-dump, fixed-target, collider, and rare-meson-decay experiments, which are summarized in Fig. 6. Reference [117] proposed an inclusive search for dark photons at LHCb based on both prompt and displaced dimuon resonances, and estimated that LHCb will have sensitivity to large regions of unexplored dark-photon parameter space by the end of Run 3 (see Fig. 6). Reference [118] is the published version of this search using Run 2 LHCb data, which confirms that the predictions for Run 3 in Ref. [117] are accurate. The sensitivity in Run 2, while already world leading, is greatly reduced due to the much smaller luminosity than expected in Run 3, and by the fact that the hardware trigger discards most of the potential signal.

In 2018, LHCb implemented electron identification in the first high-level trigger stage, which enabled developing new $A' \to e^+e^-$ triggers. The data collected by these triggers are currently being used to search for $A' \to e^+e^-$ decays—which would be mostly produced in $\pi^0 \to \gamma A'$ and $\eta \to \gamma A'$ decays—allowing LHCb to begin to exploring new parameter space below the dimuon threhold. The sensitivity using this inclusive $A' \to e^+e^-$ approach is expected to be superior to the radiative-charm method proposed in Ref. [119] in Run 3 and beyond; this is included in the future LHCb curve shown in Fig. 6.

2.8.2 Higgs portal

A similar scenario involves mass mixing between the SM Higgs and a dark-sector scalar field. Using Run 1 data [120, 121], LHCb searched for $B^0 \to K^{(*)}\chi$ with $\chi \to \mu^+\mu^-$ and placed the most stringent constraints on the Higgs portal at low masses. Reference [122] shows that the increased luminosity and improved trigger efficiency is expected to result in a sizable increase in sensitivity in future LHCb data-taking runs (the inclusion of hadronic decay modes with larger branching fractions will also improve the reach). However, the sensitivity is ultimately limited by the decay-time acceptance of LHCb, which motivates the addition of the Codex-b detector; see Ref. [123].

2.8.3 Axion-like particles

Reference [124] showed that $b \to s$ penguin decays can provide the best sensitivity to ALPs whose dominant coupling is to the gluonic field or to quarks. LHCb can perform such searches, *e.g.* $B \to Ka$ with $a \to 3\pi, \eta\pi\pi, K\overline{K}\pi$, $\phi\phi$, *etc.*, surpassing the current world-leading sensitivities. Furthermore, Refs. [125, 126] showed that $B \to KX(3\pi)$ provides excellent sensitivity to a gauged baryon-number boson. In general, $b \to s$ penguin decays provide excellent sensitivity to any non-conserved current.

2.8.4 Non-minimal scenarios

While the minimal portal models are both compelling and simple, they are not the only viable dark-sector scenarios. Many other well-motivated dark-sector models exist, and some of these would have avoided detection in all previous experimental searches. For example, hidden-valley (HV) scenarios that exhibit confinement in the dark sector would produce a high multiplicity of light hidden hadrons from showering processes. These hidden hadrons would typically decay displaced from the *pp* collision, thus failing the criteria employed in the LHCb dark-photon searches to suppress backgrounds due to heavy-flavor quarks. To overcome such a blind spot, LHCb published more general searches [127] producing world-leading model-independent constraints. When recast for the HV scenario just mentioned, these placed the first constraints on physically relevant HV mixing strengths in the $\mathcal{O}$(GeV) mass range. For many other scenarios, the Run 2 results do not yet provide relevant constraints. As LHCb collects more data, future searches will explore larger and larger regions of dark-sector model space.

2.9 Exotic hadrons

Even almost six decades after the Quark Model proposal [128, 129], many fundamental questions about the hadronic spectrum await satisfactory resolution. For example, it is unknown if diquarks [130, 131], strongly motivated by perturbative QCD, are good building blocks for more complex quark structures like tetraquarks $((qq)(\bar{q}\bar{q}))$, pentaquarks $((qq)(qq)\bar{q})$, etc. It is also unknown if nuclear-type forces can bind mesons to other mesons $(q\bar{q}) - (q\bar{q})$ or baryons $(q\bar{q}) - (qqq)$ in "molecular" states.

Hadrons formed from heavy quarks (Q=c or b) play a special role in hadron spectroscopy by providing a clear separation of constituent masses from interaction energies. This has played out in history already twice; first with the discovery of the J/ψ [132, 133] with the other narrow charmonium states ($c\bar{c}$), and more recently with the discovery of many charmonium-like, and some bottomonium-like states, which in addition to the $Q\bar{Q}$ component contain light constituents [98, 134]. Lattice QCD simulations of such systems are handicapped by their extended sizes and often unstable nature.

In view of the poor status of the theoretical description of the newly discovered particle zoo, the progress in hadron spectroscopy has been driven in recent years by the experimental data. The LHCb experiment, with its unique capability to take advantage of the large strong heavy-quark production cross-section at the LHC, offers an unmatched window of opportunity to explore heavy hadron spectroscopy, in both the conventional and exotic sectors. A good demonstration of its power was a number of key measurements of the properties of the first heavy tetraquark candidate, the $\chi_{c1}(3872)$ state: J^{PC} [135,136]; mass, width and lineshape [137, 138]; radiative decays [139]; magnitude of isospin violation in $\pi^+\pi^- J/\psi$ decay [140]; and production properties [141–143], including surprising dependence of its prompt cross-section on pp collision multiplicity [144]. While it is clear that the $\chi_{c1}(3872)$ is not a pure charmonium state, it is still unresolved if the $\chi_{c1}(3872)$ state is a mixture of $\chi_{c1}(2^3P_1)$ state with a $D^0 - \overline{D}^{*0}$ molecule, or a compact diquark tetraquark state. The LHCb upgrades will allow a coupled-channel analysis of $\pi^+\pi^- J/\psi$, $\pi^+\pi^-\pi^0 J/\psi$ and $D^0\overline{D}^{*0}$ final states to determine the position and the nature of its resonant pole, improved determination of its radiative decays which are a key in probing for the $\chi_{c1}(2^3P_1)$ component, as well as more production studies including formation in heavy-ion collisions testing the size of the state (Sec. 2.12).

A key contribution of the LHCb experiment to hadron spectroscopy was the discovery of the $P_c^+ \to J/\psi p$ pentaquark states in $\Lambda_b^0 \to J/\psi p K^-$ decays [145, 146]. These structures were clarified with the full LHCb data to be narrow mass peaks [147], just below the $\Sigma_c^+\overline{D}^0$ and $\Sigma_c^+\overline{D}^{*0}$ thresholds (Fig. 7(left)), fueling molecular interpretations. LHCb also produced 3σ evidence for a $P_{cs}^0 \to J/\psi\Lambda$ pentaquark structure just below the $\Xi_c^0\overline{D}^{*0}$ threshold [148]. More recently, a 3.1σ evidence for a $J/\psi p$ (or $J/\psi\bar{p}$) state, not near any obvious meson-baryon threshold, was found by LHCb in $B^0 \to J/\psi p\bar{p}$ decays [149], hinting that other binding mechanisms may also be at work. Future LHCb data in these, and related channels (e.g. $\eta_c p$ [150], $\chi_{cJ} p$ [142, 151, 152]), will be crucially important for uncovering all dynamical effects in the $c\bar{c}qqq$ systems. In general, access to clean samples of heavy charmed baryons, including pentaquarks, via weak decays of b mesons and baryons will continue to be a strong advantage of the LHCb program.

After the initial evidence for $J/\psi\phi$ mass structures from CDF [154] and CMS [155], the amplitude analyses of $B^+ \to J/\psi\phi K^+$ decays by LHCb revealed a rich spectrum of $J/\psi\phi$ states [156, 157], which do not follow the pattern expected for the charmonium states, as well as the first observation of $J/\psi K^+$ states [158]. The widths of these structures are too large for a molecular interpretation, thus making them candidates for compact tetraquarks. Effects due to the coupled channels with charmed meson pairs need to be evaluated in the future. Similarly, explicitly exotic mass structures in the $c\bar{c}u\bar{d}$ quark configuration [159–164] require further investigation. One pressing question is if the narrow states, like $Z_c(3900)^+$, discovered at the e^+e^- colliders [165, 166], are produced in B meson decays at all.

The observation of the explicitly exotic $X_J(2900) \to D^-K^+$ states ($J = 0, 1$) in the LHCb amplitude analysis of $B^+ \to D^+D^-K^+$ decays [167, 168] opens a new chapter in exotic hadron spectroscopy. At this point it is not clear if these $\bar{c}\bar{s}qq$ states are compact tetraquarks or structures related to the nearby D^*K^* and D_1K thresholds. Investigation of many related B decay modes will help clarify this situation. The LHCb observation of

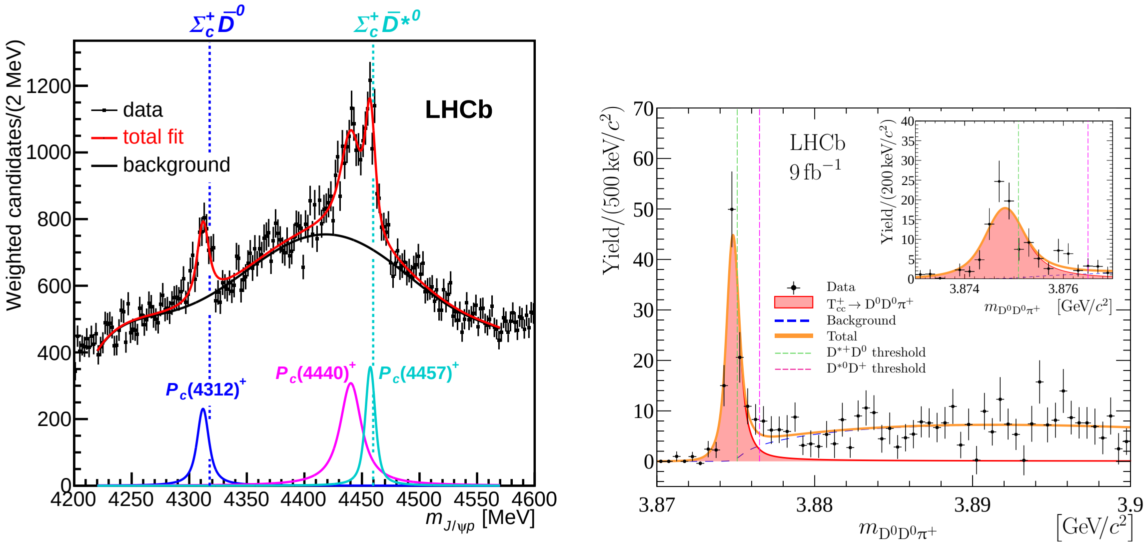

Figure 7: The LHCb observations of the narrow P_c^+ states [147] (left) and the T_{cc}^+ state [153] (right).

a significant $J/\psi J/\psi$ mass structure [169] near 6900 MeV was possibly the first spotting of compact $QQ\bar{Q}\bar{Q}$ tetraquarks. It is not clear if one or more states shape the observed mass spectrum, and the nearby $J/\psi\psi(2S)$ and $J/\psi\psi(3770)$ thresholds may also have significant impact on this structure [170]. Much larger data samples obtained with the upgraded LHCb experiment in all related charmonium-pair channels will lead to a better understanding of this sector.

The LHCb observation of the doubly-heavy Ξ_{cc} baryon [171] signaled that the data samples were reaching a level at which $cc\bar{q}\bar{q}$ states could be observed. The lightest $J^P = 1^+$ compact tetraquark in this configuration was predicted to be near the strong decay threshold [172]. The extremely narrow $T_{cc}(3875)^+$ state was recently discovered by LHCb (Fig. 7(right)) through its decay to $D^0D^0\pi^+$, only 6 MeV above the decay threshold [153, 173], fitting these expectations. Nevertheless, the molecular mechanism can also be at work here because this state is slightly below the $(DD^*)^+$ threshold. For even heavier quark combinations, with one or both c quarks replaced by b quark, the two tetraquark binding are likely to produce stable states at sufficiently different masses to be separated [174]. While T_{bb} states, with both b quarks decaying weakly, will be very difficult to isolate experimentally (see the next section), T_{bc} and T_{bs} states will be more approachable.

The Run 1-2 phase of the LHCb program has led to numerous groundbreaking discoveries, and it is natural to expect even more, often not well anticipated, exotic hadrons to be observed with the upgraded LHCb detector. In addition, many remaining questions about previous discoveries and related channels may be answered with the much larger data samples that will be collected.

2.10 Excited b and c hadron spectroscopy

LHCb has also been a discovery factory for new hadrons fitting into the conventional meson and baryon picture. To date, LHCb has discovered 55 new hadrons, as shown in

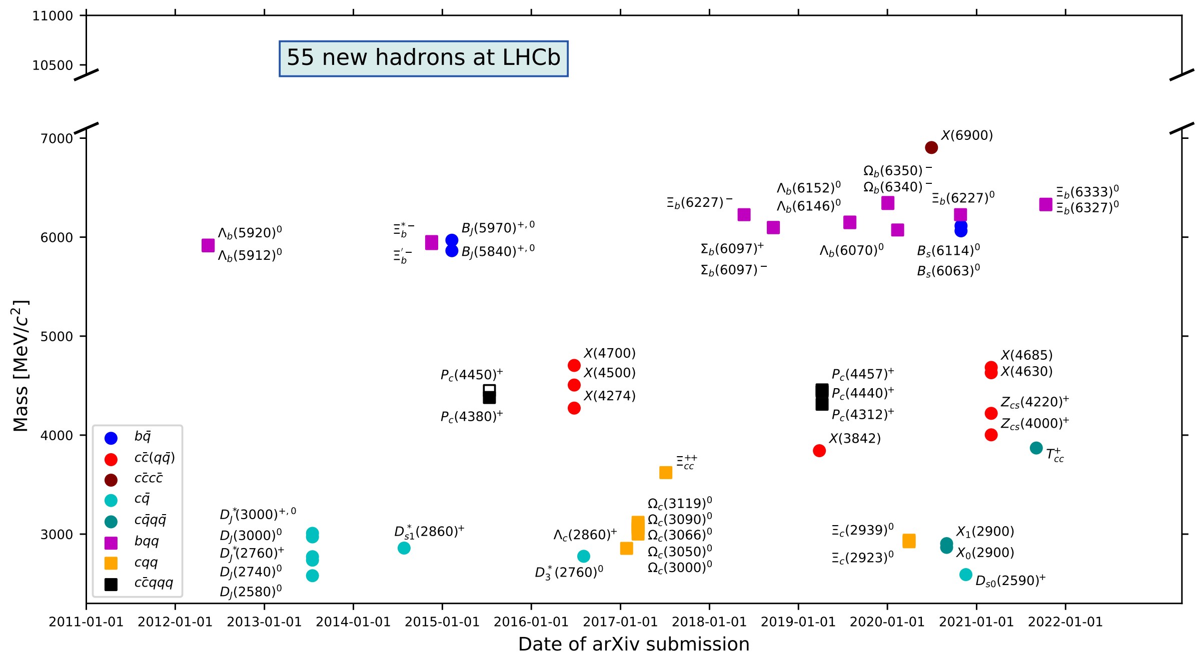

Figure 8: Graph showing the 55 new hadrons discovered by LHCb since 2011 (through the end of 2021). Seven additional hadrons have been discovered by CMS and ATLAS, not shown here.

Fig. 8. A number of additional states, not shown here, are on the cusp of observation, and the large increase in sample sizes should lead to their discovery, with more precise measurements of masses and widths, and the determination of each state's quantum numbers, when possible.

As discussed in Section 2.9, there is still much to learn about how to best describe not only exotic hadrons, but also conventional hadrons as well. The underlying theory is QCD, but QCD allows for the formation of color-singlet states in numerous ways, and how those degrees of freedom are expressed in different hadrons is still unclear. For example, the recently-discovered $D_s(2590)^+$ state – discovered by LHCb in $B^0 \to D^+D^-K^+\pi^-$ decays [175] – is conjectured to contain about 10% of D^*K in its wave function [176].

LHCb has amassed the world's largest samples of inclusively selected charm hadrons, which include the charm meson decays $D^0 \to K^-\pi^+$, $D^+ \to K^-\pi^+\pi^+$ and $D_s^+ \to K^+K^-\pi^+$, as well as the charm baryon decays $\Lambda_c^+ \to pK^-\pi^+$, $\Xi_c^0 \to pK^-K^-\pi^+$, $\Xi_c^+ \to pK^-\pi^+$ and $\Omega_c^0 \to pK^-K^-\pi^+$. With LHCb's discovery of the Ξ_{cc}^{++} [171], it is likely that future discoveries of the Ξ_{cc}^+ and Ω_{cc}^+ are just around the corner. Moreover, those inclusively selected double-charm baryons can then be used to search for and measure the properties of the excited Ξ_{cc} and Ω_{cc}^+ states.

In the beauty baryon sector, LHCb excels not only in $J/\psi \to \mu^+\mu^-$ triggered events, such as $B^- \to J/\psi K^-$, but comparable-sized samples have been collected in fully-hadronic final states, such as $B^- \to D^0\pi^-$, $B^0 \to D^-\pi^+$ and $B_s^0 \to D_s^-\pi^+$. Moreover, the world's largest samples of the beauty-baryon decays $\Lambda_b^0 \to \Lambda_c^+\pi^-(\pi^+\pi^-)$, $\Xi_b^- \to \Xi_c^0\pi^-(\pi^+\pi^-)$, $\Xi_b^0 \to \Xi_c^+\pi^-(\pi^+\pi^-)$ and $\Omega_b^- \to \Omega_c^0\pi^-(\pi^+\pi^-)$ have been recorded. With the full software trigger in the future, fully-hadronic final states will provide the largest samples of b hadrons to conduct searches for higher-mass/excited b hadrons.

For both the beauty and charm hadron samples, one or more additional particles can be combined with these ground state hadrons to observe new excited charm and beauty states. Some recent observations in just the last couple of years include the $\Xi_c(2923)^0$ and $\Xi_c(2939)^0$ baryons decaying to $\Lambda_c^+ K^-$ [177], the $\Xi_b(6227)^0$ baryon [178] in $\Xi_b^- \pi^+$, the $\Xi_b(6327)^0$ and $\Xi_b(6333)^0$ decaying to $\Lambda_b^0 K^- \pi^+$ [179], and the $\Omega_b^-(6340)^-$ and $\Omega_b^-(6350)^-$ in the $\Xi_b^0 K^-$ [180] final state (see Fig. 9). It is still an open question as to whether the multiplet of excited states in the $\Xi_c^+ K^-$ and $\Xi_b^0 K^-$ mass spectra [180–182] can be described as conventional Ω_c^0 (css) and Ω_b^- (bss) excited states. Recently two new excited B_s^0 states, $B_s(6063)^0$ and $B_s(6114)^0$ were also discovered in the B^+K^- spectrum [183]. Clearly a lot more can be done with the 10 and 50 times larger data samples expected in Upgrade I and Upgrade II, respectively.

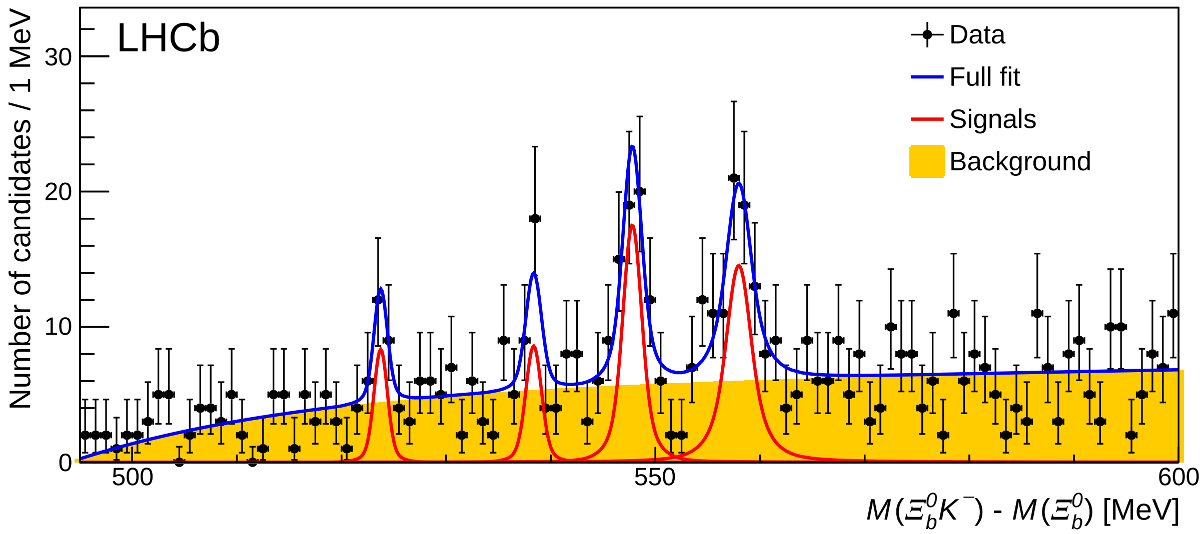

Figure 9: Invariant mass difference $M(\Xi_b^0 K^-) - M(\Xi_b^0)$ distribution for $\Xi_b^0 K^-$ combinations, showing four peaks consistent with being excited Ω_b^- states.

To search for new charm hadrons, or illuminate the properties, e.g. spin-parity, (J^P), of ones detected in prompt charm production, one can search for excited charm hadrons among the decay products of specific b-hadron decay modes. Because the J^P of the initial b-hadron is known, an amplitude analysis can be used to determine the J^P of excited charm baryons in the final state [175, 182].

Another avenue of pursuit in the LHCb upgrade will be the continued search for the double-heavy (bc) baryons, Ξ_{bc}^+ [184], Ξ_{bc}^0 [185, 186] and Ω_{bc}^0 [186]. Here, there are a multitude of possible decay modes associated with either the weak decay of the b or the c quark. With the large samples of inclusively selected and detached J/ψ, $\Xi_{cc}^{++,+}$, and $\Xi_b^{0,-}$ decays, the Ξ_{bc}^+ could be easily discovered in one of many modes, including, but not limited to $J/\psi \Xi_c^+$, $\Xi_b^0 \pi^+$, and $\Xi_{cc}^{++} \pi^-$. A rough estimate would give an expected signal of about 600 $\Xi_{bc}^+ \to J/\psi \Xi_c^+$ decays with the samples expected to be collected in Upgrade II [1]. Searches for double-beauty (bb) baryons are also of interest in the LHCb upgrade. Full reconstruction of two beauty hadrons results in very low rates due to the small branching fractions. However, a potential signature that circumvents this issue would be to observe a signal for B_c^+ decays that come from a displaced vertex [187]. Additional information would be needed to disentangle the contributions of double-beauty baryons

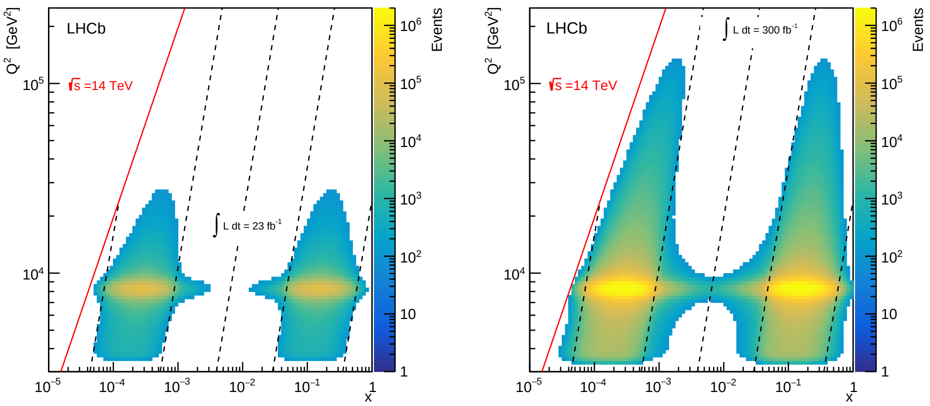

Figure 10: The regions probed in the $x - Q^2$ plane with Z boson measurements at LHCb in 14 TeV proton-proton collisions. Integrated luminosities considered are (left) a dataset of 23 fb^{-1}, considering only dimuon final states and (right) 300 fb^{-1}, considering both dimuon and dielectron final states. The solid red line shows the kinematic limit set by the collision energy; the dashed lines show the values of x and Q^2 associated with Z bosons with zero transverse momentum, and rapidities of 0, 2, and 4.5.

from double-beauty tetraquarks, if a signal was to be observed.

2.11 Forward electroweak and high-p_{T} QCD measurements

The unique forward acceptance and excellent charged particle reconstruction of the LHCb detector allows for a rich program of precision electroweak and high-p_{T} QCD measurements that can probe the Standard Model at the energy frontier. With the planned calorimeter upgrade, electron reconstruction at high-p_{T} will no longer be limited by ECAL saturation and a similar reconstruction precision for electrons and muons is expected. We summarize here briefly some of the interesting top quark and gauge boson measurements that can be made by LHCb for HL-LHC; further details can be found in Section 8 of Ref. [1].

Top quark measurements in the forward region at LHC [188, 189] can test SM theory predictions—such as the $t\bar{t}$ charge asymmetry, which is predicted to rise from 1% in the central region to 8% within the LHCb acceptance—and constrain PDF uncertainties, particularly at large Bjorken-x values. For example, measuring the inclusive $t\bar{t}$ cross section with a precision of 4% can reduce by over 20% the gluon PDF uncertainty at large x [190]. With the LHCb Upgrade II detector and accompanying dataset, differential $t\bar{t}$ measurements will also be possible, which will impose even more stringent constraints.

The HL-LHC dataset will also allow double-differential measurements of Z boson production as a function of rapidity and dilepton invariant mass to be made with high statistical precision, setting important constraints on PDFs across the $x - Q^2$ phase space, as illustrated in Fig. 10. Further constraints can be obtained from gauge boson + heavy flavor measurements (e.g. Ref. [191]), and others.

The effective weak mixing angle, usually parametrized as $\sin^2\theta_{\mathrm{W}}^{\mathrm{eff}}$, is a fundamental parameter of the Standard Model and can be determined experimentally from forward-backward asymmetries in Z boson production. In the forward acceptance of LHCb, this asymmetry is larger and easier to measure, and Z boson production is better constrained theoretically; LHCb has previously measured $\sin^2\theta_{\mathrm{W}}^{\mathrm{eff}}$ from Run 1 [192]. The most precise determinations of this quantity have been made by the LEP and SLD collaborations, but there is a difference between these of almost three standard deviations, which will be important to resolve. With Upgrade II, the expected performance of LHCb should result in a precise enough measurement of $\sin^2\theta_{\mathrm{W}}^{\mathrm{eff}}$ to probe the LEP/SLD tension.

A precise direct measurement of the W boson mass can probe the detailed theory of electroweak symmetry breaking in the Standard Model. The 2020 PDG world average for direct measurements of the W mass has a total uncertainty of ± 12 MeV, but measurements from hadron colliders are now limited in precision by theoretical uncertainties in the modelling of W boson production. It was pointed out in Ref. [193] that a W mass measurement by LHCb could reduce the overall uncertainty in combination with the CMS+ATLAS measurements, because of partial cancellation in the PDF uncertainty based on the complementary pseudorapidity regions. LHCb published a direct measurement of m_W in 2021 [194], achieving an uncertainty of ± 23 (statistical), ± 10 (experimental), ± 17 (theory) and ± 9 (PDF) MeV. With the Upgrade II dataset, a statistical precision of a few MeV should be reached, and the systematic uncertainties further constrained, leading to a precise m_W measurement from LHCb, and significant improvement in the world average.

2.12 Heavy ion physics

LHCb pursues a unique heavy ion physics program that incorporates both beam+beam and fixed-target collisions. The combination of forward coverage, precision vertexing, full particle identification, and a fast DAQ gives LHCb unique capabilities for both small and large ion collisions. There is interest in future expansions of the LHCb fixed-target program to include a spin polarized gas target [195], which would expand the physics reach of the LHC complex, or solid targets [196].

The forward rapidity coverage of LHCb and high collision energy provides access to the lowest Bjorken x values that can be probed in the laboratory, while the capability to reconstruct tracks at very low p_{T} allows the low Q^2 region to be studied in detail. This combination of low x and low Q^2 uniquely positions LHCb to quantify potential signatures of gluon saturation in the nucleus [197]. In particular, relatively rare probes such as direct photon+hadron correlations will be measured with precision to place new constraints on the saturation scale and various models of the color-glass condensate. Significant samples of ultraperipheral AA and pA events will also be accumulated in future runs, enabling new measurements of bottomonia states to place further constraints on nuclear parton distribution functions, as well as new searches for exotic states, new phenomena, and BSM particles [198–200].

The charmonium and bottomonium states accessible in dilepton decays, such as $J/\psi, \psi(2S)$ and the $\Upsilon(nS)$ resonances, will be measured precisely by the end of Run 3. However, interpreting the suppressing effects of color screening on these states is complicated by significant feed down from higher quarkonia states [201, 202], and requires the influence of quark coalescence to be quantified [203, 204]. LHCb will pursue measurements of P-wave charmonium states χ_{c1} and χ_{c2} in central AA collisions, and compare this to LHCb measurements from fixed target Pb+gas collisions, where the charm cross-section, and therefore coalescence effects, are much smaller. Tens of thousands of these χ_c states are expected per nb^{-1} of integrated PbPb luminosity. LHCb has the potential to measure

P-wave bottomonium states and separate them with high precision, which would allow for a systematic study of the bottomonium family and their relative feed down, which is crucial to constrain color screening in deconfined plasma. Expected count rates for χ_b states are in the hundreds per nb^{-1}, depending on the lower bound of achievable p_{T} coverage.

LHCb's precision vertexing capability and low p_{T} coverage, combined with the forward boost of b hadrons, provides new opportunities to measure b hadron species in a kinematic range where energy loss effects in quark gluon plasma are especially prevalent. Measurements of b hadrons in AA collisions will give new information on the transport properties of the deconfined medium and hadronization following deconfinement [205, 206]. The ability to reject the large prompt backgrounds in heavy ion collisions will allow the B_s^0 and B_c^+ mesons, as well as b baryons, to be fully reconstructed down to low p_{T}. Projections based on existing data show that thousands of B_s^0 and hundreds B_c^+ mesons should be counted per nb^{-1} of integrated PbPb luminosity.

Coalescence in heavy ion collisions can also enhance production of exotic multiquark hadrons [207–209]. LHCb measurements at low p_{T} will be uniquely sensitive to coalescence of thermalized quarks into these exotic states. In particular, measurements of the $\chi_{c1}(3872)$ tetraquark, the P_c^+ pentaquarks, and the fully charmed tetraquark $X(6900)$ in central PbPb collisions will be pursued. In addition to providing new constraints on the allowed structures of hadrons, models of statistical hadronization and coalescence can be tested in a totally new regime of number of constituent quarks. Projections from existing preliminary pPb data show that ~ 1000 $\chi_{c1}(3872)$ counts are expected per nb^{-1} of integrated PbPb luminosity, although in AA collisions this may be significantly modified by quark-gluon plasma effects.

3 Future upgrades of LHCb

Operating LHCb at the higher instantaneous luminosity needed to reach the LHCb Upgrade II physics goals requires a complete upgrade of the detector. This upgrade should maintain and extend the strengths of the experiment, including the flexible software trigger from Upgrade I. Approximately 40 interactions per bunch crossing are expected in the Upgrade II era, leading to extremely high detector occupancy and irradiation, while heavy ion collisions produce even larger numbers of particles in the detector. To meet these challenges, detector R&D is required to choose between different potential technologies. Details of the detector requirements, and technology options that may meet them, have been presented in the Framework TDR [2]. In analogy with the current LHCb Upgrade, whose physics run is imminent, the Upgrade II physics goals require major changes to nearly all the detector components. This will involve a program of development of novel technologies, some of which will likely be deployed in future HEP experiments.

The LHCb detector comprises a state of the art tracking system, complemented by particle identification components that identify hadrons, muons and electrons, and reconstruct the energies and momenta of photons and π^0 and η mesons. A unique feature that will be implemented in the current upgrade is the software trigger that relies on fast pattern recognition and reconstruction. Maintaining this capability in Upgrade II is crucial. While fast reconstruction of charged particle trajectories and neutral particle clusters are key ingredients of this algorithm, precision timing measurements from multiple sub-detectors are also required to associate the reconstructed objects to the right primary vertex.

The detector envisaged for Upgrade II maintains the footprint of the LHCb Upgrade I detector shown in Fig. 1. The tracking system will consist of a Vertex Locator (VELO) and tracking stations (Upstream Tracker or UT) placed upstream of the dipole magnet, tracking stations mounted on the magnet side walls, and a downstream tracking system composed of an outer section instrumented with scintillating fiber with a silicon pixel innermost section (Mighty Tracker or MT). The magnet side chambers are an addition to the Upgrade I detector configuration that will allow improved efficiency for the reconstruction of low momentum charged particles. The PID system is composed by two Ring Imaging Cherenkov detectors (RICH1 and RICH2) for hadron identification, an electromagnetic calorimeter (ECAL) and four muon stations (M2-M5). In addition, a time-of-flight detector (TORCH) is planned to be installed in front of RICH2 in order to better discrimination the pion-kaon-proton hypotheses at low momentum. The design does not include an hadron calorimeter (HCAL), which will allow the installation of a muon shield necessary to remove the additional punch-through background.

The key requirements to be addressed in the R&D program leading to the final detector design are:

1. Radiation hard technologies beyond the ones adopted for the current upgrade. For example, the VELO sensors and electronics need to withstand a radiation dose up to 400 MRad per year in the innermost section. The ECAL is expected to withstand up to 100 MRad in the innermost region.

2. Detectors with a granularity adequate to cope with the higher occupancy produced in high-pileup beam crossings and central heavy ion collisions.

3. Integration of the timing information in the detector readout to be able to associate hits with the right primary vertex.

The integration of timing information in the hits recorded by different subdetectors deserves particular attention. The *pp* collisions in one bunch crossing occur over a time span of approximately 1 ns, with $\mathcal{O}(10\,\text{ps})$ between collisions. The use of timing starts with the VELO near the collision point. Tagging VELO tracks with a time resolution of 20 ps greatly reduces the combinatorial complexity involved in identifying primary and secondary vertices. Thus the current strategy is to implement the VELO detector as a full 4-dimensional tracking system.

The use of the timing information in the particle identification components is also crucial. Here there are three main detector systems involved: the RICH1, RICH2 and TORCH for hadron identification; the ECAL for photon and π^0 reconstruction and electron identification; and the muon stations. Time measurements on the order of 10 ps allow matching between these detectors and particular interactions in each beam crossing. This greatly reduces the number of track–photon combinations to be considered in the RICH reconstruction, and is crucial for separating signals in the ECAL from background energy deposits. Timing is also utilized for PID in the TORCH, where time-of-flight enables positive identification of kaons and protons below 10 GeV.

The UT and downstream tracking stations are optimized with particular emphasis to the increased occupancy, which is addressed with a significant increase of the segmentation of the sensor design in the upgraded UT, and with the introduction of highly segmented silicon tracking stations in the regions of highest occupancy of the SciFi planes. The improved granularity also has benefits in the software trigger system, reducing the number of potential combinations during pattern recognition. In both of these silicon subdetectors, monolithic active pixel sensors may allow coverage of the required area with enough granularity.

The achievement of the desired performance in the RICH detectors relies on the development of high granularity and high efficiency SiPM devices featuring sufficient radiation hardness. An interesting R&D theme is the investigation into the use of metamaterials, such as photonic crystals, as a RICH radiator. These have several potential advantages, such as a short radiator length, and if demonstrated to be a realisable solution could be a transformative technology for Upgrade II.

A baseline calorimeter concept encompasses an inner portion based on crystal and plastic scintillation fibers (SpaCal), to achieve the desired radiation hardness, surrounded by a Shashlik calorimeter with moderate segmentation. In order to improve the timing performance, additions of timing layers at the location of approximate shower maximum, separating the front from the back sections are studied. In addition, an alternative silicon-based calorimeter, featuring high granularity and full 5D information is being studied. This R&D activity is very synergistic with efforts to develop particle-flow calorimeters for future HEP detectors.

The significant increase in the number of channels for all the detector system, of total radiation dose, and addition of timing information for several components is well aligned with the basic research needs in front end ASIC development [210]. In addition, the massive amount of data being moved from detector components requires careful planning of the data aggregation and transmission, with possible deployment of local intelligence, such as FPGA processor constructing four-dimensional tracking segments [211]. Similarly, cluster finding algorithms and data aggregation from different front-end ASICs could simplify the connectivity challenge in high granularity systems.

4 Data acquisition and online processing

LHCb has been upgraded for Run 3, and as part of this upgrade, the trigger is moving to a fully software-based implementation that will operate at the full LHC bunch crossing rate. This fully software-based trigger will maintain the high efficiencies for muonic signatures at the increased Run 3 luminosity, while also increasing efficiency for hadronic signatures by a factor of two—despite the harsher Run 3 environment. The data volume will be about 32 Tb per second, comparable to what the ATLAS and CMS software triggers must process during HL-LHC running starting in Run 4. Therefore, designing and delivering a fully software-based trigger for LHCb already in Run 3 has been one of the biggest computing challenges in particle physics since the previous Snowmass process.

As in Runs 1 and 2, the software trigger will consist of two stages. The first stage involves a fully GPU-based implementation, referred to as Allen, that can process the 32 Tb/s data rate and perform a wide variety of pattern recognition tasks [212]. These tasks include finding the trajectories of charged particles, finding pp collision points, identifying particles as hadrons or leptons, and finding the displaced decay vertices of long-lived particles. Allen is the first complete high-throughput GPU trigger proposed for a particle-physics experiment. As in Run 2, the data selected by the first stage will be buffered on disk while a full offline-quality detector alignment and calibration are performed. Subsequently the second stage, which will be implemented on CPUs, will perform a full offline-quality reconstruction and an array of physics selections [213]. The data stream will be made up almost entirely of online-reconstructed particles, with most low-level information discarded to reduce the event size.

At the targeted instantaneous luminosity for Runs 5 and 6, the LHCb detector will produce roughly 200 Tb of data per second. This huge data volume will need to be processed in real time and reduced by a factor of $\mathcal{O}(10^4)$ before being sent to permanent storage. A paradigm shift will be required in the LHCb trigger strategy because the expected 40 pp interactions per bunch crossing will produce multiple heavy-flavor hadrons in the LHCb detector acceptance in each event. Therefore, it will no longer be sufficient to select bunch crossings that contain inclusive heavy-flavor signatures such as displaced vertices. Instead, a strategy of pile-up suppression will be employed, where detector hits not associated with the pp interaction of interest are discarded as early as possible.

Timing information will be critical for fast categorization of reconstructed objects according to pp collision. In addition, a processor farm will need to be built using whatever the most commercially viable technologies are at the start of Run 5. Considering the recent trend towards more heterogeneous computing architectures, and the increasing prevalence of GPU and FPGA accelerators, it will be critical to continue pursuing R&D to ensure that LHCb algorithms can take advantage of the most affordable architecture then—whatever that happens to be.

References

[1] LHCb collaboration, *Physics case for an LHCb Upgrade II — Opportunities in flavour physics, and beyond, in the HL-LHC era*, `arXiv:1808.08865`.

[2] LHCb collaboration, *LHCb Framework TDR for the LHCb Upgrade II Opportunities in flavour physics, and beyond, in the HL-LHC era*, CERN-LHCC-2021-012, 2022.

[3] L. Silvestrini, *Effective Theories for Quark Flavour Physics*, in *Les Houches summer school: EFT in Particle Physics and Cosmology*, 2019, `arXiv:1905.00798`; J. F. Kamenik, *Flavour physics and CP violation*, in *2014 European School of High-Energy Physics*, 79–94, 2016, `arXiv:1708.00771`; G. Isidori, Y. Nir, and G. Perez, *Flavor Physics Constraints for Physics Beyond the Standard Model*, Ann. Rev. Nucl. Part. Sci. **60** (2010) 355, `arXiv:1002.0900`.

[4] LHCb collaboration, R. Aaij *et al.*, *Measurement of the $B_s^0 \to \mu^+\mu^-$ decay properties and search for the $B^0 \to \mu^+\mu^-$ and $B_s^0 \to \mu^+\mu^-\gamma$ decays*, Phys. Rev. **D105** (2022) 012010, `arXiv:2108.09283`.

[5] LHCb collaboration, R. Aaij *et al.*, *Simultaneous determination of CKM angle γ and charm mixing parameters*, JHEP **12** (2021) 141, `arXiv:2110.02350`.

[6] LHCb collaboration, R. Aaij *et al.*, *Test of lepton universality in beauty-quark decays*, `arXiv:2103.11769`, to appear in Nature Physics.

[7] LHCb collaboration, R. Aaij *et al.*, *Observation of CP violation in charm decays*, Phys. Rev. Lett. **122** (2019) 211803, arXiv:1903.08726.

[8] LHCb collaboration, R. Aaij *et al.*, *Search for dark photons produced in 13 TeV pp collisions*, Phys. Rev. Lett. **120** (2018) 061801, arXiv:1710.02867.

[9] LHCb collaboration, R. Aaij *et al.*, *Search for the lepton-flavour violating decays* $B^+ \to K^+\mu^\pm e^\mp$, Phys. Rev. Lett. **123** (2019) 231802, arXiv:1909.01010.

[10] LHCb collaboration, *Framework TDR for the LHCb Upgrade: Technical Design Report*, CERN-LHCC-2012-007, 2012.

[11] LHCb collaboration, *LHCb VELO Upgrade Technical Design Report*, CERN-LHCC-2013-021, 2013.

[12] LHCb collaboration, *LHCb PID Upgrade Technical Design Report*, CERN-LHCC-2013-022, 2013.

[13] LHCb collaboration, *LHCb Tracker Upgrade Technical Design Report*, CERN-LHCC-2014-001, 2014.

[14] LHCb collaboration, *LHCb Trigger and Online Upgrade Technical Design Report*, CERN-LHCC-2014-016, 2014.

[15] LHCb collaboration, *LHCb Upgrade Software and Computing*, CERN-LHCC-2018-007, 2018.

[16] LHCb collaboration, *Computing Model of the Upgrade LHCb experiment*, CERN-LHCC-2018-014, 2018.

[17] C. L. Da Siva, *Magnet side stations*, Presented at 4th Workshop on LHCb Upgrade II, 2020.

[18] Belle-II collaboration, W. Altmannshofer *et al.*, *The Belle II Physics Book*, PTEP **2019** (2019) 123C01, Erratum ibid. **2020** (2020) 029201, arXiv:1808.10567.

[19] LHCb collaboration, R. Aaij *et al.*, *Test of lepton universality with* $B^0 \to K^{*0}\ell^+\ell^-$ *decays*, JHEP **08** (2017) 055, arXiv:1705.05802.

[20] LHCb collaboration, R. Aaij *et al.*, *Measurement of CP violation in* $B^0 \to J/\psi K^0_S$ *and* $B^0 \to \psi(2S)K^0_S$ *decays*, JHEP **11** (2017) 170, arXiv:1709.03944.

[21] LHCb collaboration, R. Aaij *et al.*, *Updated measurement of time-dependent CP-violating observables in* $B^0_s \to J/\psi K^+K^-$ *decays*, Eur. Phys. J. **C79** (2019) 706, Erratum ibid. **C80** (2020) 601, arXiv:1906.08356.

[22] ATLAS collaboration, *ATLAS B-physics studies at increased LHC luminosity, potential for CP-violation measurement in the* $B^0_s \to J/\psi\phi$ *decay*, ATL-PHYS-PUB-2013-010.

[23] LHCb collaboration, R. Aaij *et al.*, *Measurement of the CP-violating phase* ϕ_s *in* $\overline{B}^0_s \to D^+_s D^-_s$ *decays*, Phys. Rev. Lett. **113** (2014) 211801, arXiv:1409.4619.

[24] LHCb collaboration, R. Aaij *et al.*, *Measurement of CP violation in $B_s^0 \to \phi\phi$ decays*, Phys. Rev. **D90** (2014) 052011, arXiv:1407.2222.

[25] CMS collaboration, *ECFA 2016: Prospects for selected standard model measurement with the CMS experiment at the High-Luminosity LHC*, CMS-PAS-FTR-14-015.

[26] LHCb collaboration, R. Aaij *et al.*, *Measurement of the CP asymmetry in B_s^0–$\overline{B}_s^0$ mixing*, Phys. Rev. Lett. **117** (2016) 061803, arXiv:1605.09768.

[27] LHCb collaboration, R. Aaij *et al.*, *Determination of the quark coupling strength $|V_{ub}|$ using baryonic decays*, Nature Physics **11** (2015) 743, arXiv:1504.01568.

[28] LHCb collaboration, R. Aaij *et al.*, *Analysis of neutral B-meson decays into two muons*, Phys. Rev. Lett. **128** (2022) 041801, arXiv:2108.09284.

[29] CMS collaboration, *Study of $B \to \mu^+\mu^-$ decays as a physics benchmark for the CMS Phase-II upgrade*, CMS-PAS-FTR-14-015.

[30] LHCb collaboration, R. Aaij *et al.*, *Measurement of the ratio of branching fractions $\mathcal{B}(\overline{B}^0 \to D^{*+}\tau^-\overline{\nu}_\tau)/\mathcal{B}(\overline{B}^0 \to D^{*+}\mu^-\overline{\nu}_\mu)$*, Phys. Rev. Lett. **115** (2015) 111803, Publisher's Note ibid. **115** (2015) 159901, arXiv:1506.08614.

[31] LHCb collaboration, R. Aaij *et al.*, *Test of lepton flavor universality by the measurement of the $B^0 \to D^{*-}\tau^+\nu_\tau$ branching fraction using three-prong τ decays*, Phys. Rev. **D97** (2018) 072013, arXiv:1711.02505.

[32] LHCb collaboration, R. Aaij *et al.*, *Measurement of the ratio of branching fractions $\mathcal{B}(B_c^+ \to J/\psi\tau^+\nu_\tau)/\mathcal{B}(B_c^+ \to J/\psi\mu^+\nu_\mu)$*, Phys. Rev. Lett. **120** (2018) 121801, arXiv:1711.05623.

[33] LHCb collaboration, R. Aaij *et al.*, *Search for time-dependent CP violation in $D^0 \to K^+K^-$ and $D^0 \to \pi^+\pi^-$ decays*, Phys. Rev. **D104** (2021) 072010, arXiv:2105.09889.

[34] LHCb collaboration, R. Aaij *et al.*, *Observation of the mass difference between neutral charm-meson eigenstates*, Phys. Rev. Lett. **127** (2021) 111801, arXiv:2106.03744.

[35] A. Cerri *et al.*, *Report from Working Group 4: Opportunities in Flavour Physics at the HL-LHC and HE-LHC*, CERN Yellow Rep. Monogr. **7** (2019) 867, arXiv:1812.07638.

[36] J. Charles *et al.*, *New physics in b meson mixing: Future sensitivity and limitations*, Phys. Rev. **D102** (2020) 056023, These and additional plots can be found at the CKMFitter group's web page.

[37] A. D. Sakharov, *Violation of CP Invariance, C asymmetry, and baryon asymmetry of the universe*, Pisma Zh. Eksp. Teor. Fiz. **5** (1967) 32.

[38] A. Giri, Y. Grossman, A. Soffer, and J. Zupan, *Determining γ using $B^\pm \to DK^\pm$ with multibody D decays*, Phys. Rev. **D68** (2003) 054018.

[39] M. Gronau and D. Wyler, *On determining a weak phase from charged B decay asymmetries*, Physics Letters **B265** (1991) 172.

[40] D. Atwood, I. Dunietz, and A. Soni, *Enhanced CP Violation with* $B \to \mathrm{KD}^0(\overline{D}^0)$ *Modes and Extraction of the Cabibbo-Kobayashi-Maskawa Angle* γ, Phys. Rev. Lett. **78** (1997) 3257.

[41] D. Atwood, I. Dunietz, and A. Soni, *Improved methods for observing* CP *violation in* $B^\pm \to KD$ *and measuring the CKM phase* γ, Phys. Rev. **D63** (2001) 036005.

[42] CKMfitter Group, J. Charles *et al.*, *Current status of the standard model CKM fit and constraints on* $\Delta F = 2$ *new physics*, Phys. Rev. **D91** (2015) 073007.

[43] LHCb collaboration, R. Aaij *et al.*, *Measurement of the CP-violating phase* ϕ_s *from* $B^0_s \to J/\psi\pi^+\pi^-$ *decays in 13 TeV pp collisions*, Phys. Lett. **B797** (2019) 134789, arXiv:1903.05530.

[44] M. Bartsch, G. Buchalla, and C. Kraus, $B \to V_L V_L$ *Decays at Next-to-Leading Order in QCD*, arXiv:0810.0249.

[45] M. Beneke, J. Rohrer, and D. Yang, *Branching fractions, polarisation and asymmetries of* $B \to VV$ *decays*, Nuclear Physics **B774** (2007) 64.

[46] H.-Y. Cheng and C.-K. Chua, *QCD factorization for charmless hadronic* B_s *decays revisited*, Phys. Rev. **D80** (2009) 114026.

[47] LHCb collaboration, R. Aaij *et al.*, *Amplitude analysis of the* $B^0_{(s)} \to K^{*0}\overline{K}^{*0}$ *decays and measurement of the branching fraction of the* $B^0 \to K^{*0}\overline{K}^{*0}$ *decay*, JHEP **07** (2019) 032, arXiv:1905.06662.

[48] A. J. Buras and E. Venturini, *Searching for New Physics in Rare* K *and* B *Decays without* $|V_{cb}|$ *and* $|V_{ub}|$ *Uncertainties*, arXiv:2109.11032.

[49] C. T. Sachrajda *et al.*, *Radiative corrections to semileptonic decay rates*, PoS **LATTICE2019** (2019) 162, arXiv:1910.07342.

[50] Fermilab Lattice, MILC collaboration, W. I. Jay *et al.*, *B- and D-meson semileptonic decays with highly improved staggered quarks*, in *38th International Symposium on Lattice Field Theory*, 2021, arXiv:2111.05184.

[51] M. Bordone, B. Capdevila, and P. Gambino, *Three loop calculations and inclusive Vcb*, Phys. Lett. **B822** (2021) 136679, arXiv:2107.00604.

[52] M. Bona, *Updates in the unitarity triangle fits with UT fit*, Presented at ICHEP, Prague, Czech Republic, 2020.

[53] LHCb collaboration, R. Aaij *et al.*, *First observation of the decay* $B^0_s \to K^-\mu^+\nu_\mu$ *and measurement of* $|V_{ub}|/|V_{cb}|$, Phys. Rev. Lett. **126** (2021) 081804, arXiv:2012.05143.

[54] LHCb collaboration, R. Aaij *et al.*, *Test of lepton universality in beauty-quark decays*, arXiv:2103.11769.

[55] LHCb collaboration, R. Aaij *et al.*, *Tests of lepton universality using $B^0 \to K^0_S \ell^+\ell^-$ and $B^+ \to K^{*+}\ell^+\ell^-$ decays*, arXiv:2110.09501.

[56] LHCb collaboration, R. Aaij *et al.*, *Test of lepton universality with $B^0 \to K^{*0}\ell^+\ell^-$ decays*, JHEP **08** (2017) 055, arXiv:1705.05802.

[57] LHCb collaboration, R. Aaij *et al.*, *Test of lepton universality with $\Lambda^0_b \to pK^-\ell^+\ell^-$ decays*, JHEP **05** (2020) 040, arXiv:1912.08139.

[58] LHCb collaboration, R. Aaij *et al.*, *Measurement of CP-Averaged Observables in the $B^0 \to K^{*0}\mu^+\mu^-$ Decay*, Phys. Rev. Lett. **125** (2020) 011802, arXiv:2003.04831.

[59] LHCb collaboration, R. Aaij *et al.*, *Angular Analysis of the $B^+ \to K^{*+}\mu^+\mu^-$ Decay*, Phys. Rev. Lett. **126** (2021) 161802, arXiv:2012.13241.

[60] ATLAS collaboration, M. Aaboud *et al.*, *Angular analysis of $B^0_d \to K^*\mu^+\mu^-$ decays in pp collisions at $\sqrt{s} = 8$ TeV with the ATLAS detector*, JHEP **10** (2018) 047, arXiv:1805.04000.

[61] CMS collaboration, A. M. Sirunyan *et al.*, *Measurement of angular parameters from the decay $\mathrm{B}^0 \to \mathrm{K}^{*0}\mu^+\mu^-$ in proton-proton collisions at $\sqrt{s} = 8$ TeV*, Phys. Lett. **B781** (2018) 517, arXiv:1710.02846.

[62] Belle collaboration, S. Wehle *et al.*, *Lepton-Flavor-Dependent Angular Analysis of $B \to K^*\ell^+\ell^-$*, Phys. Rev. Lett. **118** (2017) 111801, arXiv:1612.05014.

[63] LHCb collaboration, R. Aaij *et al.*, *Branching Fraction Measurements of the Rare $B^0_s \to \phi\mu^+\mu^-$ and $B^0_s \to f_2'(1525)\mu^+\mu^-$- Decays*, Phys. Rev. Lett. **127** (2021) 151801, arXiv:2105.14007.

[64] T. Hurth, F. Mahmoudi, D. M. Santos, and S. Neshatpour, *More indications for lepton nonuniversality in $b \to s\ell^+\ell^-$*, Phys. Lett. **B824** (2022) 136838, arXiv:2104.10058.

[65] BaBar collaboration, J. P. Lees *et al.*, *Evidence for an excess of $\bar{B} \to D^{(*)}\tau^-\bar{\nu}_\tau$ decays*, Phys. Rev. Lett. **109** (2012) 101802, arXiv:1205.5442.

[66] Belle collaboration, M. Huschle *et al.*, *Measurement of the branching ratio of $\bar{B} \to D^{(*)}\tau^-\bar{\nu}_\tau$ relative to $\bar{B} \to D^{(*)}\ell^-\bar{\nu}_\ell$ decays with hadronic tagging at Belle*, Phys. Rev. **D92** (2015) 072014, arXiv:1507.03233.

[67] LHCb collaboration, R. Aaij *et al.*, *Measurement of the ratio of branching fractions $\mathcal{B}(\bar{B}^0 \to D^{*+}\tau^-\bar{\nu}_\tau)/\mathcal{B}(\bar{B}^0 \to D^{*+}\mu^-\bar{\nu}_\mu)$*, Phys. Rev. Lett. **115** (2015) 111803, arXiv:1506.08614, [Addendum: Phys. Rev. Lett.115,no.15,159901(2015)].

[68] Belle collaboration, Y. Sato *et al.*, *Measurement of the branching ratio of $\bar{B}^0 \to D^{*+}\tau^-\bar{\nu}_\tau$ relative to $\bar{B}^0 \to D^{*+}\ell^-\bar{\nu}_\ell$ decays with semileptonic tagging*, Phys. Rev. **D94** (2016) 072007, arXiv:1607.07923.

[69] Belle collaboration, S. Hirose *et al.*, *Measurement of the τ lepton polarization and $R(D^*)$ in the decay $\bar{B} \to D^*\tau^-\bar{\nu}_\tau$*, Phys. Rev. Lett. **118** (2017) 211801, arXiv:1612.00529.

[70] Belle collaboration, G. Caria *et al.*, *Measurement of $\mathcal{R}(D)$ and $\mathcal{R}(D^*)$ with a semileptonic tagging method*, Phys. Rev. Lett. **124** (2020) 161803, arXiv:1910.05864.

[71] LHCb collaboration, R. Aaij *et al.*, *Observation of the decay $\Lambda_b^0 \to \Lambda_c^+\tau^-\bar{\nu}_\tau$*, LHCb-PAPER-2021-044,CERN-EP-2021-265, in preparation.

[72] R. R. Horgan, Z. Liu, S. Meinel, and M. Wingate, *Rare B decays using lattice QCD form factors*, PoS **LATTICE2014** (2015) 372, arXiv:1501.00367.

[73] LATTICE-HPQCD collaboration, J. Harrison, C. T. H. Davies, and A. Lytle, *$R(J/\psi)$ and $B_c^- \to J/\psi\ell^-\bar{\nu}_\ell$ Lepton Flavor Universality Violating Observables from Lattice QCD*, Phys. Rev. Lett. **125** (2020) 222003, arXiv:2007.06956.

[74] F. U. Bernlochner, Z. Ligeti, D. J. Robinson, and W. L. Sutcliffe, *Precise predictions for $\Lambda_b \to \Lambda_c$ semileptonic decays*, Phys. Rev. **D99** (2019) 055008, arXiv:1812.07593.

[75] W. Altmannshofer and D. M. Straub, *New physics in $b \to s$ transitions after LHC run 1*, Eur. Phys. J. **C75** (2015) 382, arXiv:1411.3161.

[76] HFLAV collaboration, Y. S. Amhis *et al.*, *Averages of b-hadron, c-hadron, and τ-lepton properties as of 2018*, arXiv:1909.12524, updated results and plots available at https://hflav.web.cern.ch/.

[77] M. Beneke, C. Bobeth, and R. Szafron, *Power-enhanced leading-logarithmic QED corrections to $B_q \to \mu^+\mu^-$*, JHEP **10** (2019) 232, arXiv:1908.07011.

[78] P. Koppenburg, *Flavour Anomalies*, , https://www.nikhef.nl/~pkoppenb/anomalies.html.

[79] LHCb collaboration, R. Aaij *et al.*, *Tests of lepton universality using $B^0 \to K_S^0\ell^+\ell^-$ and $B^+ \to K^{*+}\ell^+\ell^-$ decays*, arXiv:2110.09501, submitted to PRL.

[80] LHCb collaboration, R. Aaij *et al.*, *Angular analysis of the rare decay $B_s^0 \to \phi\mu^+\mu^-$*, JHEP **11** (2021) 043, arXiv:2107.13428.

[81] LHCb collaboration, R. Aaij *et al.*, *Angular moments of the decay $\Lambda_b^0 \to \Lambda\mu^+\mu^-$ at low hadronic recoil*, JHEP **09** (2018) 146, arXiv:1808.00264.

[82] S. Bifani, S. Descotes-Genon, A. Romero Vidal, and M.-H. Schune, *Review of Lepton Universality tests in B decays*, J. Phys. G **46** (2019) 023001, arXiv:1809.06229.

[83] F. U. Bernlochner, M. Franco Sevilla, D. J. Robinson, and G. Wormser, *Semitauonic b-hadron decays: A lepton flavor universality laboratory*, Rev. Mod. Phys. **94** (2022) 015003, arXiv:2101.08326.

[84] LHCb collaboration, R. Aaij *et al.*, *Measurement of the ratio of branching fractions $\mathcal{B}(B_c^+ \to J/\psi\tau^+\nu_\tau)/\mathcal{B}(B_c^+ \to J/\psi\mu^+\nu_\mu)$*, Phys. Rev. Lett. **120** (2018) 121801, arXiv:1711.05623.

[85] LHCb collaboration, R. Aaij *et al.*, *Observation of the decay $\Lambda_b^0 \to \Lambda_c^+\tau^-\overline{\nu}_\tau$*, arXiv:2201.03497.

[86] N. Serra, R. Silva Coutinho, and D. van Dyk, *Measuring the breaking of lepton flavor universality in $B \to K^* \ell^+ \ell^-$*, Phys. Rev. D **95** (2017) 035029, `arXiv:1610.08761`.

[87] D. Bečirević, S. Fajfer, I. Nišandžić, and A. Tayduganov, *Angular distributions of $\bar{B} \to D^{(*)} \ell \bar{\nu}_\ell$ decays and search of New Physics*, Nucl. Phys. B **946** (2019) 114707, `arXiv:1602.03030`.

[88] A. K. Alok, D. Kumar, S. Kumbhakar, and S. U. Sankar, *D^* polarization as a probe to discriminate new physics in $\bar{B} \to D^* \tau \bar{\nu}$*, Phys. Rev. D **95** (2017) 115038, `arXiv:1606.03164`.

[89] D. Hill, M. John, W. Ke, and A. Poluektov, *Model-independent method for measuring the angular coefficients of $B^0 \to D^* \tau \nu$ decays*, Journal of High Energy Physics **2019** (2019) .

[90] C. Bobeth *et al.*, *$B_{s,d} \to l^+ l^-$ in the Standard Model with reduced theoretical uncertainty*, Phys. Rev. Lett. **112** (2014) 101801, `arXiv:1311.0903`.

[91] LHCb collaboration, R. Aaij *et al.*, *Analysis of neutral B-meson decays into two muons*, Phys. Rev. Lett. **128** (2022) 041801, `arXiv:2108.09284`.

[92] LHCb collaboration, R. Aaij *et al.*, *Measurement of the $B_s^0 \to \mu^+ \mu^-$ decay properties and search for the $B^0 \to \mu^+ \mu^-$ and $B_s^0 \to \mu^+ \mu^- \gamma$ decays*, Phys. Rev. **D105** (2022) 012010, `arXiv:2108.09283`.

[93] ATLAS collaboration, M. Aaboud *et al.*, *Study of the rare decays of B_s^0 and B^0 mesons into muon pairs using data collected during 2015 and 2016 with the ATLAS detector*, JHEP **04** (2019) 098, `arXiv:1812.03017`.

[94] CMS collaboration, A. M. Sirunyan *et al.*, *Measurement of properties of $B_\mathrm{s}^0 \to \mu^+ \mu^-$ decays and search for $B^0 \to \mu^+ \mu^-$ with the CMS experiment*, JHEP **04** (2020) 188, `arXiv:1910.12127`.

[95] LHCb collaboration, R. Aaij *et al.*, *Search for the decays $B_s^0 \to \tau^+ \tau^-$ and $B^0 \to \tau^+ \tau^-$*, Phys. Rev. Lett. **118** (2017) 251802, `arXiv:1703.02508`.

[96] LHCb collaboration, R. Aaij *et al.*, *Search for the Rare Decays $B_s^0 \to e^+ e^-$ and $B^0 \to e^+ e^-$*, Phys. Rev. Lett. **124** (2020) 211802, `arXiv:2003.03999`.

[97] LHCb collaboration, R. Aaij *et al.*, *Precise measurement of the f_s/f_d ratio of fragmentation fractions and of B_s^0 decay branching fractions*, Phys. Rev. **D104** (2021) 032005, `arXiv:2103.06810`.

[98] Particle Data Group, P. A. Zyla *et al.*, *Review of Particle Physics*, PTEP **2020** (2020) 083C01.

[99] K. De Bruyn *et al.*, *Probing New Physics via the $B_s^0 \to \mu^+ \mu^-$ Effective Lifetime*, Phys. Rev. Lett. **109** (2012) 041801, `arXiv:1204.1737`.

[100] R. Barbieri, G. Isidori, A. Pattori, and F. Senia, *Anomalies in B-decays and $U(2)$ flavour symmetry*, Eur. Phys. J. **C76** (2016) 67, `arXiv:1512.01560`.

[101] M. Bordone, C. Cornella, J. Fuentes-Martín, and G. Isidori, *A three-site gauge model for flavor hierarchies and flavor anomalies*, Phys. Lett. **B779** (2018) 317, arXiv:1712.01368.

[102] M. Bordone, C. Cornella, J. Fuentes-Martín, and G. Isidori, *Low-energy signatures of the* PS^3 *model: from B-physics anomalies to LFV*, JHEP **10** (2018) 148, arXiv:1805.09328.

[103] M. Duraisamy, S. Sahoo, and R. Mohanta, *Rare semileptonic* $B \to K(\pi) l_i^- l_j^+$ *decay in a vector leptoquark model*, Phys. Rev. **D95** (2017) 035022, arXiv:1610.00902.

[104] L. Di Luzio, A. Greljo, and M. Nardecchia, *Gauge leptoquark as the origin of B-physics anomalies*, Phys. Rev. **D96** (2017) 115011, arXiv:1708.08450.

[105] L. Di Luzio *et al.*, *Maximal flavour violation: a Cabibbo mechanism for leptoquarks*, JHEP **11** (2018) 081, arXiv:1808.00942.

[106] LHCb collaboration, R. Aaij *et al.*, *Search for the lepton-flavour-violating decays* $B_s^0 \to \tau^\pm \mu^\mp$ *and* $B^0 \to \tau^\pm \mu^\mp$, Phys. Rev. Lett. **123** (2019) 211801, arXiv:1905.06614.

[107] LHCb collaboration, R. Aaij *et al.*, *Search for the lepton flavour violating decay* $B^+ \to K^+ \mu^- \tau^+$ *using* B_{s2}^{*0} *decays*, JHEP **06** (2020) 129, arXiv:2003.04352.

[108] BaBar collaboration, J. P. Lees *et al.*, *A search for the decay modes* $B^\pm \to h^\pm \tau \ell$, Phys. Rev. **D86** (2012) 012004, arXiv:1204.2852.

[109] M. Borsato *et al.*, *Effective-field-theory arguments for pursuing lepton-flavor-violating K decays at LHCb*, Phys. Rev. **D99** (2019) 055017, arXiv:1808.02006.

[110] A. A. Alves Junior *et al.*, *Prospects for measurements with strange hadrons at LHCb*, JHEP **05** (2019) 048, arXiv:1808.03477.

[111] LHCb collaboration, R. Aaij *et al.*, *Search for the rare decay* $K_{\mathrm{S}}^0 \to \mu^+\mu^-$, JHEP **01** (2013) 090, arXiv:1209.4029.

[112] LHCb collaboration, R. Aaij *et al.*, *Evidence for the rare decay* $\Sigma^+ \to p\mu^+\mu^-$, Phys. Rev. Lett. **120** (2018) 221803, arXiv:1712.08606.

[113] HyperCP collaboration, H. Park *et al.*, *Evidence for the decay* $\Sigma^+ \to p\mu^+\mu^-$, Phys. Rev. Lett. **94** (2005) 021801, arXiv:hep-ex/0501014.

[114] F. Dettori, D. Martinez Santos, and J. Prisciandaro, *Low-*p_T *dimuon triggers at LHCb in Run 2*, , LHCb-PUB-2017-023, CERN-LHCb-PUB-2017-023.

[115] LHCb collaboration, R. Aaij *et al.*, *Constraints on the* $K_{\mathrm{S}}^0 \to \mu^+\mu^-$ *branching fraction*, Phys. Rev. Lett. **125** (2020) 1231801, arXiv:2001.10354.

[116] M. Graham, C. Hearty, and M. Williams, *Searches for dark photons at accelerators*, Annual Review of Nuclear and Particle Science **71** (2021) arXiv:2104.10280.

[117] P. Ilten *et al.*, *Proposed inclusive dark photon search at LHCb*, Phys. Rev. Lett. **116** (2016) 251803, arXiv:1603.08926.

[118] LHCb collaboration, R. Aaij *et al.*, *Search for $A' \to \mu^+\mu^-$ decays*, Phys. Rev. Lett. **124** (2020) 041801, arXiv:1910.06926.

[119] P. Ilten, J. Thaler, M. Williams, and W. Xue, *Dark photons from charm mesons at LHCb*, Phys. Rev. **D92** (2015) 115017, arXiv:1509.06765.

[120] LHCb collaboration, R. Aaij *et al.*, *Search for hidden-sector bosons in $B^0 \to K^{*0}\mu^+\mu^-$ decays*, Phys. Rev. Lett. **115** (2015) 161802, arXiv:1508.04094.

[121] LHCb collaboration, R. Aaij *et al.*, *Search for long-lived scalar particles in $B^+ \to K^+\chi(\mu^+\mu^-)$ decays*, Phys. Rev. **D95** (2017) 071101, arXiv:1612.07818.

[122] LHCb collaboration, R. Aaij *et al.*, *Physics case for an LHCb Upgrade II - Opportunities in flavour physics, and beyond, in the HL-LHC era*, arXiv:1808.08865.

[123] G. Aielli *et al.*, *Expression of interest for the CODEX-b detector*, Eur. Phys. J. **C80** (2020) 1177, arXiv:1911.00481.

[124] D. Aloni, Y. Soreq, and M. Williams, *Coupling QCD-Scale Axionlike Particles to Gluons*, Phys. Rev. Lett. **123** (2019) 031803, arXiv:1811.03474.

[125] J. A. Dror, R. Lasenby, and M. Pospelov, *New constraints on light vectors coupled to anomalous currents*, Phys. Rev. Lett. **119** (2017) 141803, arXiv:1705.06726.

[126] J. A. Dror, R. Lasenby, and M. Pospelov, *Dark forces coupled to nonconserved currents*, Phys. Rev. **D96** (2017) 075036, arXiv:1707.01503.

[127] LHCb collaboration, R. Aaij *et al.*, *Searches for low-mass dimuon resonances*, JHEP **10** (2020) 156, arXiv:2007.03923.

[128] M. Gell-Mann, *A schematic model of baryons and mesons*, Phys. Lett. **8** (1964) 214.

[129] G. Zweig, *An SU_3 model for strong interaction symmetry and its breaking*, CERN-TH-401, 1964.

[130] D. B. Lichtenberg and L. J. Tassie, *Baryon mass splitting in a boson-fermion model*, Phys. Rev. **155** (1967) 1601.

[131] R. L. Jaffe, *Exotica*, Physics Reports **409** (2005) 1.

[132] E598 collaboration, J. J. Aubert *et al.*, *Experimental observation of a heavy particle J*, Phys. Rev. Lett. **33** (1974) 1404.

[133] SLAC-SP-017 collaboration, J. E. Augustin *et al.*, *Discovery of a narrow resonance in e^+e^- annihilation*, Phys. Rev. Lett. **33** (1974) 1406, [Adv. Exp. Phys.5,141(1976)].

[134] S. L. Olsen, T. Skwarnicki, and D. Zieminska, *Nonstandard heavy mesons and baryons: Experimental evidence*, Rev. Mod. Phys. **90** (2018) 015003, arXiv:1708.04012.

[135] LHCb collaboration, R. Aaij *et al.*, *Determination of the $X(3872)$ meson quantum numbers*, Phys. Rev. Lett. **110** (2013) 222001, arXiv:1302.6269.

[136] LHCb collaboration, R. Aaij *et al.*, *Quantum numbers of the $X(3872)$ state and orbital angular momentum in its $\rho^0 J/\psi$ decays*, Phys. Rev. **D92** (2015) 011102(R), arXiv:1504.06339.

[137] LHCb collaboration, R. Aaij *et al.*, *Study of the line shape of the $\chi_{c1}(3872)$ state*, Phys. Rev. **D102** (2020) 092005, arXiv:2005.13419.

[138] LHCb collaboration, R. Aaij *et al.*, *Study of the $\psi_2(3823)$ and $\chi_{c1}(3872)$ states in $B^+ \to (J/\psi\pi^+\pi^-)K^+$ decays*, JHEP **08** (2020) 123, arXiv:2005.13422.

[139] LHCb collaboration, R. Aaij *et al.*, *Evidence for the decay $X(3872) \to \psi(2S)\gamma$*, Nucl. Phys. **B886** (2014) 665, arXiv:1404.0275.

[140] LHCb collaboration, R. Aaij *et al.*, *Observation of ω contribution in the $X(3872) \to \pi^+\pi^- J/\psi$ decays*, LHCb-PAPER-2021-045, in preparation.

[141] LHCb collaboration, R. Aaij *et al.*, *Measurement of $\chi_{c1}(3872)$ production in proton-proton collisions at $\sqrt{s} = 8$ and 13 TeV*, JHEP **01** (2022) 131, arXiv:2109.07360.

[142] LHCb collaboration, R. Aaij *et al.*, *Observation of the $\Lambda_b^0 \to \chi_{c1}(3872)pK^-$ decay*, JHEP **09** (2019) 028, arXiv:1907.00954.

[143] LHCb collaboration, R. Aaij *et al.*, *Observation of $X(3872)$ production in pp collisions at $\sqrt{s} = 7$ TeV*, Eur. Phys. J. **C72** (2012) 1972, arXiv:1112.5310.

[144] LHCb collaboration, R. Aaij *et al.*, *Modification of $\chi_{c1}(3872)$ and $\psi(2S)$ production in pp collisions at $\sqrt{s} = 8$ TeV*, Phys. Rev. Lett. **126** (2021) 092001, arXiv:2009.06619.

[145] LHCb collaboration, R. Aaij *et al.*, *Observation of $J/\psi p$ resonances consistent with pentaquark states in $\Lambda_b^0 \to J/\psi pK^-$ decays*, Phys. Rev. Lett. **115** (2015) 072001, arXiv:1507.03414.

[146] LHCb collaboration, R. Aaij *et al.*, *Model-independent evidence for $J/\psi p$ contributions to $\Lambda_b^0 \to J/\psi pK^-$ decays*, Phys. Rev. Lett. **117** (2016) 082002, arXiv:1604.05708.

[147] LHCb collaboration, R. Aaij *et al.*, *Observation of a narrow pentaquark state, $P_c(4312)^+$, and of two-peak structure of the $P_c(4450)^+$*, Phys. Rev. Lett. **122** (2019) 222001, arXiv:1904.03947.

[148] LHCb collaboration, R. Aaij *et al.*, *Evidence of a $J/\psi\Lambda$ structure and observation of excited Ξ^- states in the $\Xi_b^- \to J/\psi\Lambda K^-$ decay*, Science Bulletin **66** (2021) 1278, arXiv:2012.10380.

[149] LHCb collaboration, R. Aaij *et al.*, *Evidence for a new structure in the $J/\psi p$ and $J/\psi\bar{p}$ systems in $B_s^0 \to J/\psi p\bar{p}$ decays*, arXiv:2108.04720, submitted to PRL.

[150] LHCb collaboration, R. Aaij *et al.*, *First observation of the decay $\Lambda_b^0 \to \eta_c(1S)pK^-$*, Phys. Rev. **D102** (2020) 112012, arXiv:2007.11292.

[151] LHCb collaboration, R. Aaij *et al.*, *Observation of the decays $\Lambda_b^0 \to \chi_{c1} p K^-$ and $\Lambda_b^0 \to \chi_{c2} p K^-$*, Phys. Rev. Lett. **119** (2017) 062001, arXiv:1704.07900.

[152] LHCb collaboration, R. Aaij *et al.*, *Observation of the decay $\Lambda_b^0 \to \chi_{c1} p \pi^-$*, JHEP **05** (2021) 095, arXiv:2103.04949.

[153] LHCb collaboration, R. Aaij *et al.*, *Observation of an exotic narrow doubly charmed tetraquark*, arXiv:2109.01038, submitted to journal.

[154] CDF collaboration, T. Aaltonen *et al.*, *Evidence for a narrow near-threshold structure in the $J/\psi\phi$ mass spectrum in $B^+ \to J/\psi\phi K^+$ decays*, Phys. Rev. Lett. **102** (2009) 242002, arXiv:0903.2229.

[155] CMS collaboration, S. Chatrchyan *et al.*, *Observation of a peaking structure in the $J/\psi\phi$ mass spectrum from $B^\pm \to J/\psi\phi K^\pm$ decays*, Phys. Lett. **B734** (2014) 261, arXiv:1309.6920.

[156] LHCb collaboration, R. Aaij *et al.*, *Observation of exotic $J/\psi\phi$ structures from amplitude analysis of $B^+ \to J/\psi\phi K^+$ decays*, Phys. Rev. Lett. **118** (2017) 022003, arXiv:1606.07895.

[157] LHCb collaboration, R. Aaij *et al.*, *Amplitude analysis of $B^+ \to J/\psi\phi K^+$ decays*, Phys. Rev. **D95** (2017) 012002, arXiv:1606.07898.

[158] LHCb collaboration, R. Aaij *et al.*, *Observation of new resonances decaying to $J/\psi K^+$ and $J/\psi\phi$* , Phys. Rev. Lett. **127** (2021) 082001, arXiv:2103.01803.

[159] Belle collaboraation collaboration, S. K. Choi *et al.*, *Observation of a resonance-like structure in the $\pi^\pm\psi'$ mass distribution in exclusive $B \to K\pi^\pm\psi'$ decays*, Phys. Rev. Lett. **100** (2008) 142001, arXiv:0708.1790.

[160] Belle collaboration, R. Mizuk *et al.*, *Observation of two resonance-like structures in the $\pi^+\chi_{c1}$ mass distribution in exclusive $\overline{B}^0 \to K^-\pi^+\chi_{c1}$ decays*, Phys. Rev. **D78** (2008) 072004, arXiv:0806.4098.

[161] LHCb collaboration, R. Aaij *et al.*, *Observation of the resonant character of the $Z(4430)^-$ state*, Phys. Rev. Lett. **112** (2014) 222002, arXiv:1404.1903.

[162] Belle collaboration, K. Chilikin *et al.*, *Observation of a new charged charmonium-like state in $\bar{B}^0 \to J/\psi K^-\pi^+$ decays*, Phys. Rev. **D90** (2014) 112009, arXiv:1408.6457.

[163] LHCb collaboration, R. Aaij *et al.*, *Evidence for a $\eta_c(1S)\pi^-$ resonance in $B^0 \to \eta_c(1S)K^+\pi^-$ decays*, Eur. Phys. J. **C78** (2018) 1019, arXiv:1809.07416.

[164] LHCb collaboration, R. Aaij *et al.*, *Model-independent observation of exotic contributions to $B^0 \to J/\psi K^+\pi^-$ decays*, Phys. Rev. Lett. **122** (2019) 152002, arXiv:1901.05745.

[165] BESIII collaboration, M. Ablikim *et al.*, *Observation of a charged charmonium-like structure in $e^+e^- \to \pi^+\pi^- J/\psi$ at $\sqrt{s}$ =4.26 GeV*, Phys. Rev. Lett. **110** (2013) 252001, arXiv:1303.5949.

[166] Belle collaboration, Z. Q. Liu *et al.*, *Study of $e^+e^- \to \pi^+\pi^- J/\psi$ and observation of a charged charmonium-like state at Belle*, Phys. Rev. Lett. **110** (2013) 252002, Erratum ibid. **111** (2013) 019901, `arXiv:1304.0121`.

[167] LHCb collaboration, R. Aaij *et al.*, *Amplitude analysis of the $B^+ \to D^+D^-K^+$ decay*, Phys. Rev. **D102** (2020) 112003, `arXiv:2009.00026`.

[168] LHCb collaboration, R. Aaij *et al.*, *Model-independent study of structure in $B^+ \to D^+D^-K^+$ decays*, Phys. Rev. Lett. **125** (2020) 242001, `arXiv:2009.00025`.

[169] LHCb collaboration, R. Aaij *et al.*, *Observation of structure in the J/ψ-pair mass spectrum*, Science Bulletin **65** (2020) 1983, `arXiv:2006.16957`.

[170] X.-K. Dong *et al.*, *Coupled-channel interpretation of the LHCb double-J/ψ spectrum and hints of a new state near the $J/\psi J/\psi$ threshold*, Phys. Rev. Lett. **126** (2021) 132001, Erratum ibid. **127** (2021) 119901, `arXiv:2009.07795`.

[171] LHCb collaboration, R. Aaij *et al.*, *Observation of the doubly charmed baryon Ξ_{cc}^{++}*, Phys. Rev. Lett. **119** (2017) 112001, `arXiv:1707.01621`.

[172] M. Karliner and J. L. Rosner, *Discovery of doubly-charmed Ξ_{cc} baryon implies a stable $(bb\bar{u}\bar{d})$ tetraquark*, Phys. Rev. Lett. **119** (2017) 202001, `arXiv:1707.07666`.

[173] LHCb collaboration, R. Aaij *et al.*, *Study of the doubly charmed tetraquark T_{cc}^+*, `arXiv:2109.01056`, submitted to journal.

[174] Q. Meng *et al.*, *Stable double-heavy tetraquarks: spectrum and structure*, Phys. Lett. **B814** (2021) 136095, `arXiv:2009.14493`.

[175] LHCb collaboration, R. Aaij *et al.*, *Observation of a new excited D_s^+ state in $B^0 \to D^-D^+K^+\pi^-$ decays*, Phys. Rev. Lett. **126** (2021) 122002, `arXiv:2011.09112`.

[176] J.-M. Xie, M.-Z. Liu, and L.-S. Geng, *$D_{s0}(2590)$ as a dominant $c\bar{s}$ state with a small D^*K component*, Phys. Rev. **D104** (2021) 094051, `arXiv:2108.12993`.

[177] LHCb collaboration, R. Aaij *et al.*, *Observation of new Ξ_c^0 baryons decaying to $\Lambda_c^+K^-$*, Phys. Rev. Lett. **124** (2020) 222001, `arXiv:2003.13649`.

[178] LHCb collaboration, R. Aaij *et al.*, *Observation of a new Ξ_b^0 state*, Phys. Rev. **D103** (2021) 012004, `arXiv:2010.14485`.

[179] LHCb collaboration, R. Aaij *et al.*, *Observation of two new excited Ξ_b^0 states decaying to $\Lambda_b^0K^-\pi^+$*, `arXiv:2110.04497`, submitted to PRL.

[180] LHCb collaboration, R. Aaij *et al.*, *First observation of excited Ω_b^- states*, Phys. Rev. Lett. **124** (2020) 082002, `arXiv:2001.00851`.

[181] LHCb collaboration, R. Aaij *et al.*, *Observation of five new narrow Ω_c^0 states decaying to $\Xi_c^+K^-$*, Phys. Rev. Lett. **118** (2017) 182001, `arXiv:1703.04639`.

[182] LHCb collaboration, R. Aaij *et al.*, *Observation of excited Ω_c^0 baryons in $\Omega_b^- \to {\Xi_c}^+K^-\pi^+$ decays*, Phys. Rev. **D104** (2021) L091102, `arXiv:2107.03419`.

[183] LHCb collaboration, R. Aaij *et al.*, *Observation of new excited B_s^0 states*, Eur. Phys. J. C **81** (2021) 601, arXiv:2010.15931.

[184] LHCb collaboration, R. Aaij *et al.*, *Search for the doubly heavy baryon Ξ_{bc}^+ decaying to $J/\psi\Xi_c^+$,* LHCb-PAPER-2022-005, in preparation.

[185] LHCb collaboration, R. Aaij *et al.*, *Search for the doubly heavy baryon $\varXi_{bc}$ in the D^0pK^- final state*, JHEP **11** (2020) 095, arXiv:2009.02481.

[186] LHCb collaboration, R. Aaij *et al.*, *Search for the doubly heavy baryons $\varOmega_{bc}^0$ and $\varXi_{bc}^0$ decaying to $\varLambda_c^+\pi^-$ and $\varXi_c^+\pi^-$*, Chin. Phys. **C45** (2021) 093002, arXiv:2104.04759.

[187] T. Gershon and A. Poluektov, *Displaced B_c^- mesons as an inclusive signature of weakly decaying double beauty hadrons*, JHEP **01** (2019) 019, arXiv:1810.06657.

[188] LHCb collaboration, R. Aaij *et al.*, *Measurement of forward top pair production in the dilepton channel in pp collisions at $\sqrt{s}$ = 13 TeV*, JHEP **08** (2018) 174, arXiv:1803.05188.

[189] LHCb collaboration, R. Aaij *et al.*, *First observation of top quark production in the forward region*, Phys. Rev. Lett. **115** (2015) 112001, arXiv:1506.00903.

[190] R. Gauld, *Feasibility of top quark measurements at LHCb and constraints on the large-x gluon PDF*, JHEP **02** (2014) 126, arXiv:1311.1810.

[191] LHCb collaboration, R. Aaij *et al.*, *Study of Z bosons produced in association with charm in the forward region*, arXiv:2109.08084, submitted to PRL.

[192] LHCb collaboration, R. Aaij *et al.*, *Measurement of the forward-backward asymmetry in $Z/\gamma^* \to \mu^+\mu^-$ decays and determination of the effective weak mixing angle*, JHEP **11** (2015) 190, arXiv:1509.07645.

[193] G. Bozzi, L. Citelli, M. Vesterinen, and A. Vicini, *Prospects for improving the LHC W boson mass measurement with forward muons*, Eur. Phys. J. **C75** (2015) 601, arXiv:1508.06954.

[194] LHCb collaboration, R. Aaij *et al.*, *Measurement of the W boson mass*, JHEP **01** (2022) 036, arXiv:2109.01113.

[195] C. A. Aidala *et al.*, *The LHCSpin Project*, arXiv:1901.08002.

[196] V. Pugatch, *Physics and Techniques of the Fixed Metal Microstrip Target for the LHCb Experiment*, presented at CERN-Ukraine co-operation: current state and prospects, 2018.

[197] L. D. McLerran and R. Venugopalan, *Gluon distribution functions for very large nuclei at small transverse momentum*, Phys. Rev. **D49** (1994) 3352, arXiv:hep-ph/9311205.

[198] A. Esposito, C. A. Manzari, A. Pilloni, and A. D. Polosa, *Hunting for tetraquarks in ultraperipheral heavy ion collisions*, Phys. Rev. **D104** (2021) 114029, arXiv:2109.10359.

[199] ATLAS collaboration, M. Aaboud *et al.*, *Evidence for light-by-light scattering in heavy-ion collisions with the ATLAS detector at the LHC*, Nature Phys. **13** (2017) 852, arXiv:1702.01625.

[200] CMS collaboration, A. M. Sirunyan *et al.*, *Evidence for light-by-light scattering and searches for axion-like particles in ultraperipheral PbPb collisions at* $\sqrt{s_{\rm NN}} = 5.02$ *TeV*, Phys. Lett. **B797** (2019) 134826, arXiv:1810.04602.

[201] S. Digal, P. Petreczky, and H. Satz, *Quarkonium feed down and sequential suppression*, Phys. Rev. **D64** (2001) 094015, arXiv:hep-ph/0106017.

[202] F. Karsch, D. Kharzeev, and H. Satz, *Sequential charmonium dissociation*, Phys. Lett. **B637** (2006) 75, arXiv:hep-ph/0512239.

[203] M. I. Gorenstein, A. P. Kostyuk, H. Stoecker, and W. Greiner, *Statistical coalescence model with exact charm conservation*, Phys. Lett. **B509** (2001) 277, arXiv:hep-ph/0010148.

[204] X. Zhao and R. Rapp, *Medium modifications and production of charmonia at LHC*, Nucl. Phys. **A859** (2011) 114, arXiv:1102.2194.

[205] M. Schroedter, R. L. Thews, and J. Rafelski, B_c *meson production in nuclear collisions at RHIC*, Phys. Rev. **C62** (2000) 024905, arXiv:hep-ph/0004041.

[206] Y. Liu, C. Greiner, and A. Kostyuk, B_c *meson enhancement and the momentum dependence in Pb + Pb collisions at energies available at the CERN Large Hadron Collider*, Phys. Rev. **C87** (2013) 014910, arXiv:1207.2366.

[207] ExHIC collaboration, S. Cho *et al.*, *Identifying multiquark hadrons from heavy ion collisions*, Phys. Rev. Lett. **106** (2011) 212001.

[208] ExHIC collaboration, S. Cho *et al.*, *Exotic hadrons in heavy ion collisions*, Phys. Rev. **C84** (2011) 064910.

[209] B. Wu, X. Du, M. Sibila, and R. Rapp, *X(3872) transport in heavy-ion collisions*, arXiv:2006.09945.

[210] Z. Ahmed *et al.*, *New Technologies for Discovery*, in *CPAD Instrumentation Frontier Workshop 2018: New Technologies for Discovery IV*, 2019, arXiv:1908.00194.

[211] M. Petruzzo, *A 4D real-time tracking device for the LHCb Upgrade II*, PhD thesis, Milan U., 2019.

[212] R. Aaij *et al.*, *Allen: A high level trigger on GPUs for LHCb*, Comput. Softw. Big Sci. **4** (2020) 7, arXiv:1912.09161.

[213] A. Alfonso Albero *et al.*, *Upgrade trigger selection studies*, LHCb-PUB-2019-013, CERN-LHCb-PUB-2019-013.